Identifying and interpreting regional signals in tree-ring based reconstructions of snow avalanche activity in the Goms valley (Swiss Alps)

A. Favillier, S. Guillet, J. Lopez-Saez, Florie Giacona, N. Eckert, G. Zenhäusern, J.L. Peiry, M. Stoffel, C. Corona

Quaternary Science Reviews 307 (2023) 108063

Contents lists available at ScienceDirect

Quaternary Science Reviews

journal homepage: www.elsevier.com/locate/quascirev

Identifying and interpreting regional signals in tree-ring based reconstructions of snow avalanche activity in the Goms valley (Swiss Alps)

A. Favillier [a, b, c, *], S. Guillet [b, c], J. Lopez-Saez [b, c], F. Giacona [d], N. Eckert [d], G. Zenhäusern [e], J.L. Peiry [f], M. Stoffel [b, c, g], C. Corona [a]

[a] Université Clermont Auvergne, CNRS, Université de Limoges, GEOLAB, 63000, Clermont-Ferrand, France
[b] Climate Change Impacts and Risks in the Anthropocene (C-CIA), Institute for Environmental Sciences, University of Geneva, Boulevard Carl-Vogt 66, CH-1205, Geneva, Switzerland
[c] Dendrolab.ch, Department of Earth Sciences, University of Geneva, Rue des Maraîchers 13, CH-1205, Geneva, Switzerland
[d] Univ. Grenoble Alpes, INRAE, CNRS, IRD, Grenoble INP, IGE, 38000, Grenoble, France
[e] Forschungsinstitut zur Geschichte des Alpenraums, CH-3900, Brig, Switzerland
[f] Université Clermont-Auvergne, F-63000 Clermont-Ferrand & CNRS, EDYTEM, 73000, Chambéry, France
[g] Department F.-A. Forel for Environmental and Aquatic Sciences, University of Geneva, 66 Boulevard Carl-Vogt, CH-1205, Geneva, Switzerland

ARTICLE INFO

Article history:
Received 5 December 2022
Received in revised form
20 March 2023
Accepted 23 March 2023
Available online 30 March 2023

Handling Editor: Donatella Magri

Keywords:
Snow avalanches
Tree-ring analysis
Regional snow avalanche activity
Hierarchical Bayesian modelling
Swiss Alps

ABSTRACT

One of the purposes of dendrogeomorphic studies is to provide long and continuous reconstructions of mass movements and to detect climate-induced trends in process activity. The development of regional chronologies—in which information from different sites are aggregated—is often needed to identify process–climate relations and to overcome local-scale specificities, sparse data available for individual sites and to extract a signal that is common to a larger region and possibly driven by past climate fluctuations or large-scale environmental changes. Yet, such chronologies are scarce and consensus neither exists on how to compile local data at the regional scale nor on the methods to be used to extract a common signal. In the case of snow avalanches, existing regional tree-ring studies typically included less than ten paths, and they discriminated years of high/low avalanche activity based on a regional index representing the proportion of disturbed trees in any given year. However, such an index does not account for potential non-stationarities in local tree-ring reconstructions such as e.g., time-varying sample size, decreasing dendrogeomorphic potential of trees after the occurrence of an extremely large, devastating avalanche or socio-environmental changes. Here we combine a dendrogeomorphic approach to reconstruct snow avalanche events in 11 paths located in the Goms valley (Swiss Alps) with an innovative statistical modelling approach. For each path, we compute reconstructions using a 4-step procedure to disentangle potential effects of snow avalanches from disturbance pulses in trees caused by climatic or other exogenous factors. We then process the regional dataset (spanning the period 1766–2014) within a Bayesian hierarchical spatio-temporal framework specifically designed to homogenise time series of avalanche events by i) removing trends related to the decreasing number of living trees back in time and ii) inferring robust trends in mean annual/regional avalanche activity in time and space. This contribution has the merit to introduce a methodological approach allowing rigorous extraction of common, average avalanche signals from snow avalanche paths characterized by heterogeneous process activity. Despite its stringency, we show that 11 avalanche paths may not suffice to yield a signal that is independent from the selection of couloirs. As a result, the approach also does not highlight a clear climatic control of snow avalanche activity but rather points to a complex, yet combined impact of afforestation and management strategies on reconstructed avalanches.

1. Introduction

Dendrogeomorphology (Alestalo, 1971; Stoffel et al., 2010;

* Corresponding author. Université Clermont Auvergne, CNRS, Université de Limoges, GEOLAB, 63000, Clermont-Ferrand, France.
E-mail address: adrien.favillier@unige.ch (A. Favillier).

https://doi.org/10.1016/j.quascirev.2023.108063

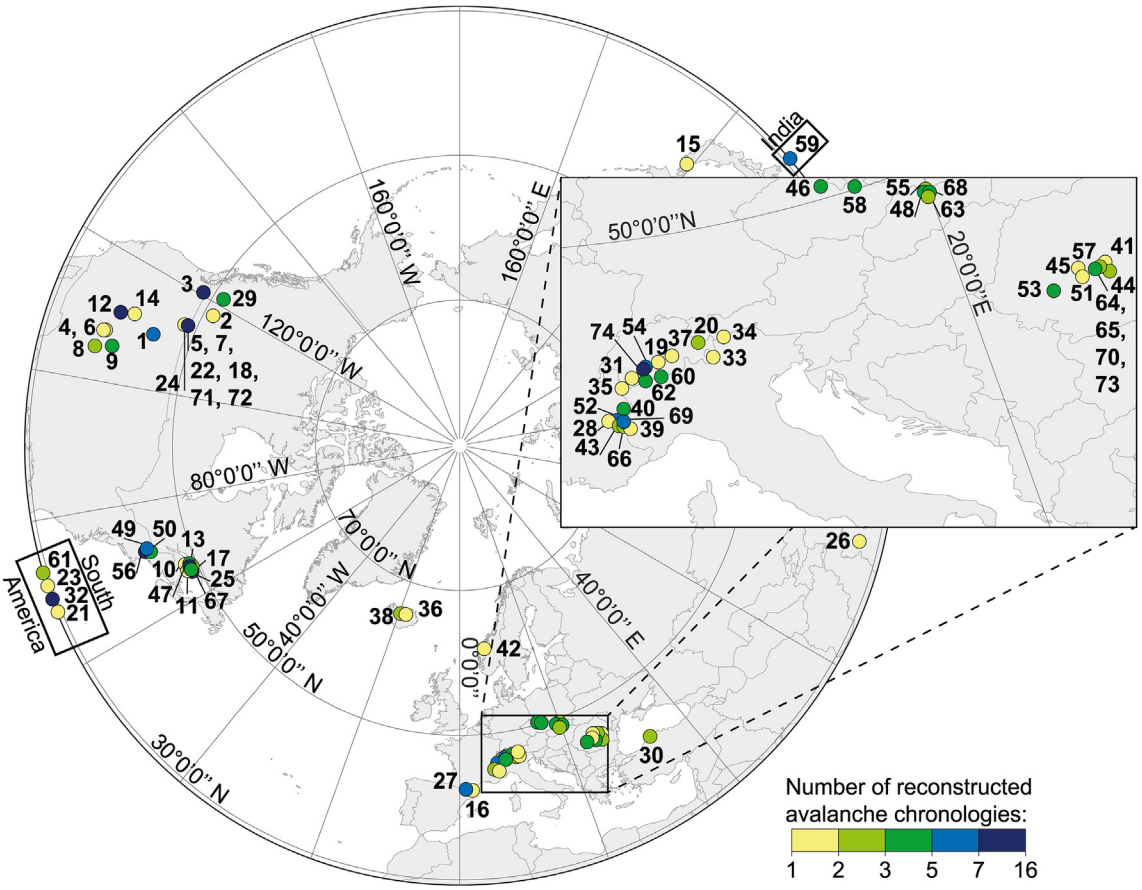

Fig. 1. Synthesis of published tree-ring based avalanche reconstructions. Colors indicate the number of paths included in the study.

Stoffel and Bollschweiler, 2008; Stoffel and Corona, 2014) is a powerful approach to reconstruct mass-movement activity at annual resolution and to provide insights into process activity over decadal to centennial time scales (Butler and Sawyer, 2008). Over the last decades, it has been used repeatedly and successfully to reconstruct past mass-movement activity such as rockfalls (Mainieri et al., 2020a; Trappmann et al., 2013; Zielonka and Wrońska-Wałach, 2019), landslides (Lopez Saez et al., 2012; Malik et al., 2016; Oven et al., 2019, Silhán and Stoffel, 2015), debris flows (Bollschweiler et al., 2008; Lopez Saez et al., 2011; Tichavský et al., 2017) and snow avalanches (Corona et al., 2012; de Bouchard d'Aubeterre et al., 2019; Favillier et al., 2018, 2017; Gratton et al., 2019; Mainieri et al., 2020b; Martin and Germain, 2016a; Schläppy et al., 2016). Basic principles of dendrogeomorphology have been established by Alestalo (1971), Shroder (1980), Butler (1987) and further refined by e.g., Stoffel and Bollschweiler (2008), Stoffel et al. (2010) or Stoffel and Corona (2014). Based on the "Process-Event-Response" concept (Shroder, 1980), the approach is based on the analysis of growth disturbances in tree-ring series (Stoffel and Bollschweiler, 2008). Cross dating of these disturbances makes it possible to reconstruct multidecadal to (multi)centennial fluctuations of mass movement activity.

A majority of dendrogeomorphic studies have so far focused on a limited number of sites. In the case of snow avalanches, an extensive survey shows that 40 out of 73 dendrogeomorphic studies listed in the literature (Fig. 1) include less than three paths. These studies are obviously useful to unveil specific spatiotemporal patterns or to allow methodological developments at a given study site. However, the sparseness of avalanche events at the path scale, the intrinsic variability of the response of each path to socio-environmental trends and methodological limitations (see below) as well as their limited spatial fingerprint has often precluded a robust detection of trends related to regional — e.g., land use and land cover changes (Mainieri et al., 2020b; Zgheib et al., 2020, 2022) or to global — e.g., climatic fluctuations (Eckert et al., 2013; Ballesteros-Cánovas et al., 2018; Giacona et al., 2021)— forcings of avalanche activity. In total, only 9 out of the 73 surveyed studies thus focused on regional reconstruction of snow avalanche activity and explored relations between climate variables and snow avalanches occurrences (Fig. 1). Schläppy et al. (2016), for instance, observed significant correlations between snowstorms and snow avalanche activity for three avalanche paths located in the Northern French Alps. In the Presidential Range (New Hampshire, USA), relying on data from 7 avalanche paths, Martin and Germain (2017) suggested that snow avalanche activity was partially controlled by the North Atlantic Oscillation via its influence on the trajectory of snowstorms. In the Indian Himalayas, Ballesteros et al. (2018) highlighted an increase in snow avalanche activity in 5 contiguous paths since the 1970s which they attributed to winter warming and changes in water content in the snowpack. Recently, Peitzsch et al. (2021b) identified a decrease in the activity of large snow avalanches in 12 snow avalanche paths in the US which seemed consistent with climate warming.

1. Potter (1969); **2.** Schaerer et al. (1972); **3.** Smith (1973); **4.** Ives et al. (1976); **5.** Butler (1979); **6.** Carrara (1979); **7.** Butler and Malanson (1985); **8.** Bryant et al. (1989); **9.** Rayback (1998); **10.**

Larocque et al. (2001); **11.** Boucher et al. (2003); **12.** Hebertson and Jenkins (2003); **13.** Dubé et al. (2004); **14.** Jenkins and Hebertson (2004); **15.** Kajimoto et al. (2004); **16.** Muntán et al. (2004); **17.** Germain et al. (2005); **18.** Pederson et al. (2006); **19.** Stoffel et al. (2006); **20.** Casteller et al. (2007); **21.** Mundo et al. (2007); **22.** Butler and Sawyer (2008); **23.** Casteller et al. (2008); **24.** Reardon et al. (2008); **25.** Germain et al. (2009); **26.** Laxton and Smith (2009); **27.** Muntán et al. (2009); **28.** Corona et al. (2010); **29.** Johnson and Smith (2010); **30.** Köse et al. (2010); **31.** Szymczak et al. (2010); **32.** Casteller et al. (2011); **33.** Garavaglia and Pelfini (2011); **34.** Kogelnig-Mayer et al. (2011); **35.** Corona et al. (2012); **36.** Decaulne et al. (2012); **37.** Püntener et al. (2012); **38.** Arbellay et al. (2013); **39.** Corona et al. (2013); **40.** Schläppy et al. (2013); **41.** Voiculescu and Onaca (2013); **42.** Decaulne et al. (2014); **43.** Schläppy et al. (2014); **44.** Voiculescu and Onaca (2014); **45.** Chiroiu et al. (2015); **46.** Tumajer and Treml (2015); **47.** Germain (2016); **48.** Lempa et al. (2016); **49.** Martin and Germain (2016a); **50.** Martin and Germain (2016b); **51.** Pop et al. (2016); **52.** Schläppy et al. (2016); **53.** Voiculescu et al. (2016); **54.** Favillier et al. (2017); **55.** Gądek et al. (2017); **56.** Martin and Germain (2017); **57.** Pop et al. (2017); **58.** Šilhán and Tichavský (2017); **59.** Ballesteros-Cánovas et al. (2018); **60.** Bollati et al. (2018); **61.** Casteller et al. (2018); **62.** Favillier et al. (2018); **63.** Krause and Křížek (2018); **64.** Meseșan et al. (2018a); **65.** Meseșan et al. (2018b); **66.** de Bouchard d'Aubeterre et al. (2019); **67.** Gratton et al. (2019); **68.** Šilhán et al. (2019); **69.** Mainieri et al. (2020a, 2020b); **70.** Todea et al. (2020); **71.** Peitzsch et al. (2021a); **72.** Peitzsch et al. (2021b); **73.** Germain et al. (2022); **74.** This study.

However, several limitations somewhat put the ability of these dendrogeomorphic studies to represent snow avalanche activity at the regional scale into question. First, (1) there is no consensus on the methods to be used to aggregate local tree-ring reconstructions into a regional chronology. Germain et al. (2005), Muntán et al. (2009) and Voiculescu et al. (2016), for example, summed up the event years retrieved at the scale of individual paths and considered the peaks in the resulting chronology to be regional events. Following the approach developed by Dubé et al. (2004), several studies (Decaulne et al., 2012, 2014; Germain et al., 2009; Martin and Germain, 2017; Peitzsch et al., 2021a, 2021b; Voiculescu et al., 2016) used a regional avalanche activity index (RAAI) computed as the ratio between the sum of local avalanche activity indices (i.e. the proportion of damaged trees in year t) and the number of paths that could have potentially recorded an avalanche in each year *t*. At the regional scale, these studies discriminate periods of high/low avalanche activity based on an arbitrary RAAI threshold ranging from 10 to 20%. In addition, (2) these studies did not account for non-stationarities that are susceptible to blur the true avalanche signal. These non-stationarities have been evidenced recently in site-specific chronologies and are intrinsic to dendrogeomorphic approaches: potential biases and noise mostly relate to time-varying sample size (Butler, 1987; Butler and Sawyer, 2008; Corona et al., 2012), the difficulty to retrieve healed injuries (Stoffel and Perret, 2006; Trappmann and Stoffel, 2013; Favillier et al., 2017) or the reduced dendrogeomorphic potential after destructive events (Corona et al., 2012; Favillier et al., 2018; Mainieri et al., 2020b). Finally, (3) land cover changes — linked to socio-economic developments such as the depopulation and land abandonment of remote mountain valleys — interfere inevitably with global warming (Mainieri et al., 2020b; Zgheib et al., 2020) but have been poorly considered to explain the reconstructed trends in avalanche activity since the mid-19th century.

To fill this gap, we propose a comprehensive approach to i) identify a robust common signal in tree-ring based reconstructions of snow avalanches and to ii) analyse to which extent this signal represents true changes in process activity and iii) whether it is driven by climate change or other drivers. To this aim, we (1) aggregated tree-ring reconstructions from 11 avalanche paths in the Goms valley (Swiss Alps) into a regional chronology. To do so, we coupled the 4-step procedure proposed by Favillier et al. (2017) that allows a robust detection of past events with an innovative Bayesian Hierarchical Logistic Regression developed specifically for this study (2) to remove trends related to the decreasing number of living trees over time. This approach yields (3) a homogenized regional reconstruction of avalanches for any given year and path without suffering from the usual sources of noise and biases as well as from local path-scale peculiarities. Hence, it reflects as much as possible the evolution of natural avalanche activity at the scale of the chosen sample of paths. We (4) discuss the strengths and weaknesses of the Bayesian Hierarchical Logistic Regression to extract a common "average" signal from a set of avalanche couloirs in the Goms Valley, and to which extent the obtained signal reflects a regional behaviour related to large scale climate change and/or socio environmental drivers rather than peculiarities of the chosen sample of paths. We notably show that 11 couloirs is too small a number to extract a truly "regional" signal because of the varying characteristics of the avalanche couloirs. We conclude that future studies should focus on even larger-scale regional reconstructions to enhance understanding of how many couloirs are needed to produce a temporal signal that becomes invariant over a given geographical area where couloirs with different shapes, process characteristics and forest stands exist.

2. Regional settings

The study sites are located in the Goms valley (Fig. 2), the uppermost part of the Rhone valley extending from the municipality of Lax to the Rhone glacier (Swiss Alps). Based on (1) the existence of old forest stands with avalanche damage, (2) the absence of possible interferences between snow avalanches and other mass movements and (3) the availability of hazard maps, three avalanche slopes were selected on the S-E facing valley slopes, namely next to and above Münster (Fig. 2b, MU, 46°29′14 N, 8°15′44 E), Geschinen (Fig. 2c, GE, 46°29′44 N, 8°16′49 E), and Oberwald (Fig. 2d, OB, 46°32′05 N, 8°20′54 E). On these slopes, 11 paths and their release area have been delineated using (1) technical reports (Geoformer 2015; in Stoffel et al., 2015; 2016a, 2016b), (2) maps of erosional and depositional avalanche features, (3) LiDAR data and aerial photographs available from the Federal Office of Topography (swisstopo). All paths exceed 1000 m in length, and cover a difference in elevation ranging from ~430 to 730 m. The characteristics of all paths are given in Table 1.

In total, four, two and five avalanche corridors have been delineated at MU (Fig. 2b), GE (Fig. 2c) and OB (Fig. 2d), respectively, with release areas ranging from 1810 to 2170 m asl. These paths directly threaten human settlements, the Matterhorn-Gotthard Bahn (MGB) railway line and the main road connecting Brig (Valais) to Andermatt (Uri). Therefore, since the 19th century, significant efforts have been undertaken to limit snow avalanche activity at the sites (Torrenté, 1888). At MU (Fig. 2b), several rows of avalanche barriers have been initially installed at MU2 and MU3 (Coaz, 1910). According to historical maps and aerial photographs (http://www.map.geo.admin.ch/, swisstopo), these protection structures were maintained and complemented with additional rows of snow bridges (MU3, MU4) in 1958, 1984, 1985, 1986, 1987, 1988, and 1998. Finally, in 1990, snow bridges and wind baffles have been installed at MU1 to prevent the formation of snow cornices. At present, 85 structures are inventoried in the release areas of MU1-MU4 (Fig. 2). At GE (Fig. 2c), wall terraces and avalanche barriers have been installed in the starting zones by the end of the 19th century (Torrenté, 1888). These structures were

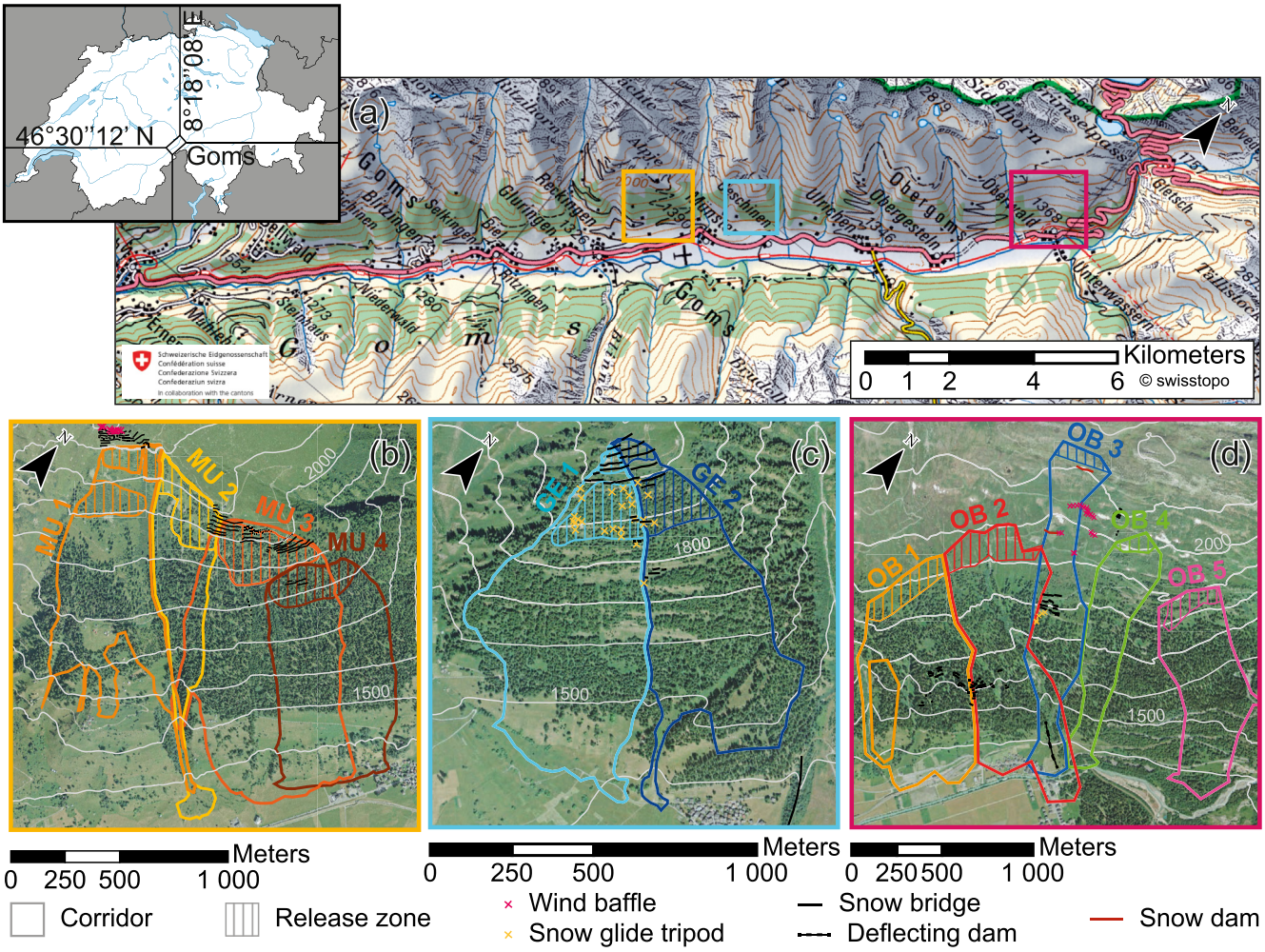

Fig. 2. Location of the study sites: (a) the Goms valley in the Canton of Valais, Switzerland, with the (b) Münster, Geschinen (c) and Oberwald (d) avalanche paths.

Table 1
Main topographic and forest characteristics of the 11 avalanche paths. Numerical values correspond to the path and release areas delineated in Fig. 1 b, c and d and derived from a 5-m DEM. Numbers in parentheses indicates trees that are located at the intersection of different avalanche paths. Please refer to the Methods section for further details about their use in the dendrogeomorphic approach.

Path	Avalanche path					Forest characteristics		
	Length (m)	Mean slope (°)	Mean slope of the release area (°)	Mean release altitude (m)	Lowest deposition altitude (m)	Sampled trees (n)	Mean age (yr)	Oldest tree (yr)
MU 1	1258	28.36	36.58	2170	1571	52 (+7)	230.5	432
MU 2	1571	29.98	40.00	2060	1390	32 (+8)	240.9	493
MU 3	1255	29.84	36.71	1941	1326	80 (+27)	225.1	513
MU 4	1000	27.79	34.28	1823	1338	50	228.4	497
GE 1	1104	32.52	38.33	2050	1388	135	146.2	554
GE 2	1147	32.49	36.87	2050	1370	140	205.2	678
OB 1	1253	27.67	27.24	1878	1363	127	235.2	584
OB 2	1562	25.90	28.16	1970	1370	135	222.6	579
OB 3	1838	26.07	33.37	2100	1368	74 (+26)	197.23	561
OB 4	1358	26.68	33.04	2018	1368	115 (+10)	188.7	584
OB 5	1155	25.38	39.06	1810	1380	74 (+3)	198.9	489
Mean	**1318.27**	**28.43**	**34.88**	**1988.18**	**1384.72**	**1014**	**205.9**	**678**

complemented with additional snow bridges and snow rakes at the beginning of the 20th century. Since the 1990s, snow bridges are no longer maintained but 29 snow rakes and 25 snow glide tripods were built between 1995 and 2006 in the southern part of the forest stand (1800–2000 m asl) to protect the village from snow avalanches. At OB (Fig. 2d), aerial photographs show that snow bridges and snow glide tripods were installed at OB3 between 1944 and 1960. In 1960, local authorities built an avalanche deflection dam in

the depositional area of avalanches flowing down paths OB2 and OB3 to protect the village. Between 1967 and 1988, rows of snow rakes have been installed on tracks OB1 and OB2 (1960–1967) and snow dams were erected at OB3 (1967–1988). Today, 84 structures prevent snow accumulation in the release zones and a dam protects the village of Oberwald (Fig. 2d).

According to the meteorological station of Ulrichen (46°5′N, 8°31′E, 1346 m asl), also in Goms valley and located between the three municipalities, annual temperature and precipitation totals are on average 3.7 °C and 1212 mm for the period 1981–2010. During winter (DJF), mean air temperature is −6.6 °C. Between November and April, precipitation mostly falls as snow with a mean annual snowfall of 578 cm over the period 1999–2010. Snow cover lasts on average 171 days.

3. Methods

3.1. Sampling strategy and detection of past avalanche events in tree-ring series

The tree-ring dataset used in this study combines the reconstructions developed at OB1-OB5 (Favillier et al., 2017) with unpublished tree-ring series collected at Münster (MU1-MU4) and Geschinen (GE1-GE2). It includes 2256 increment cores and 20 cross-sections from 1014 European Larch (*Larix decidua* Mill.) and Norway spruce (*Picea abies* (L.) Karst.). Tree-ring material was collected following the recommendations of Šilhán and Stoffel (2015) and Stoffel and Corona (2014), individual paths include a minimum of 40 (MU2) and a maximum of 140 (GE2) trees, spatially distributed on each path, and with a balanced sampling between old and young trees. A few trees are located at the intersection of paths. These trees are given in parentheses in Table 1 (MU1–MU2–MU3, MU3–MU4, OB2–OB3–OB4). Injuries (I), callus tissues (CT) (Stoffel et al., 2010), tangential rows of traumatic resin ducts (TRDs) (Schneuwly et al., 2009a, 2009b), compression wood (CW) and sharp growth suppressions (GS) (Kogelnig-Mayer et al., 2013) were dated using local reference chronologies available for the Goms valley. We classified these growth disturbances (GDs; Kogelnig-Mayer et al., 2011) according to signal strength into weak (intensity class 1), intermediate (intensity class 2), strong (intensity class 3) reactions. Injuries were considered intensity class 4. Growth disturbances detected on trees located on overlapping paths, were expertly and individually attributed to a given path consistently with annual patterns of impacted trees. To reconstruct past avalanche events, we adopted the four-step procedure proposed by Favillier et al. (2017). This procedure disentangles the potential effects of snow avalanches on tree growth from disturbance pulses caused by climatic or exogenous factors, such as cold/dry years or larch budmoth (LBM) outbreaks. The three years following an LBM outbreak (Esper et al., 2007; Büntgen et al., 2009) as well as region-specific information on extremely cold and/or dry summers (Battipaglia et al., 2010; Efthymiadis et al., 2006) were used to filter out non-avalanche signals in the reconstructions and to allocate a level of confidence to each reconstructed event (see Favillier et al., 2017, for further details). Following recommendations from Butler and Sawyer (2008), a double threshold for sample sizes of 21–54 (GD > 4 and It >5%) and 55 trees (GD > 7 and It >5%) has been used to discriminate potential avalanche and non-avalanche years in accordance with statistically determined thresholds as defined by Corona et al. (2012) for the Pelerins avalanche path (France). Based on the Wit, we then distinguish between low (LLC, Wit<0.2), medium (MLC, 0.3 >Wit>0.2), and high (HLC, Wit>0.3) levels of confidence and attribute this evaluation to the avalanche event detection. In addition, and despite the precautions taken at each of the previous step, each event detected at step 2 was rated with a LLC. Unlike the above-mentioned large-scale studies, we first reconstructed past avalanche events at the path scale before aggregation into a regional chronology.

3.2. Estimation of the regional snow avalanche activity using a hierarchical Bayesian modelling approach

3.2.1. Principle

Hierarchical Bayesian Modelling (HBM) is a flexible framework to deal with spatio-temporal data (Cressie and Wikle, 2011; Wikle et al., 1998) respecting the spatio-temporal structure of data— here, the occurrence or the absence of an avalanche in a tree-ring series for a given year. Hence, HBM does not suffer the limitations of other methods aggregating transformation of repeat observation series into a single regional series to cause an impoverishment of available data. With dependant replicates of the same “common effects” in space and time, the HBM framework thus compensates for short data series, allowing to infer robust spatio-temporal trends in mean annual/regional behaviour. For instance, the mean common temporal effect over all paths where avalanche activity has been reconstructed should be relatively free from local artefacts, thus providing a fair estimate of temporal variations of avalanche activity over the sample of studied paths. Symmetrically, the inter-annual mean local effect representing local environmental constraints (e.g., elevation) is more easily inferred with repeat observations over several years than with data corresponding to a given (annual or mean over several years) environmental condition. Eventually, HBM has the advantage of easily coping for series of uneven length, with the missing year-path couplets being simply treated as additional unknowns (Tanner, 1992). For this purpose, HBM accommodates complexity in a series of simpler conditional models which are inferred altogether, making the overall model structure much more flexible than a “traditional” Generalised Linear Model (GLM). This provides robust quantification at each sublevel of the model of the different sources of variability/uncertainty (limited quantity of available data, natural interannual and/or inter-path variability, etc.).

Here, our goal is to evaluate the probability of occurrence of at least one avalanche per year in each path in the study region in an explicit spatio-temporal framework considering limitations of tree-ring reconstructions related to the decreasing availability of dendrogeomorphic material back in time. Practically, within the HBM framework, we developed a new specific hierarchical spatio-temporal logistic regression approach to remove potential trends in tree-ring based avalanche chronologies related to the increasing number of living trees during recent decades. We thereby produced homogenized records of avalanche activity over the studied paths that can be compared to climate fluctuations or land use changes. We distinguish year-to-year and low frequency variabilities of the detrended signal using a non-parametric regression. This smoothing procedure provides more robust estimates of past changes in avalanche activity and limits the shrinkage effect inherent to hierarchical Bayesian models (i.e., the information transfer from one year to another through the inferred temporal structure), especially for the old years for which information is missing on several paths. The approach essentially adapts to tree-ring records the idea of Giacona et al. (2021) to produce a homogenized regional time series of avalanche activity from historical sources while accounting for the changing nature and number of sources over time.

3.2.2. Hierarchical Bayesian model specification

Avalanche occurrence in path i (over N paths in total) in year t (over T years in total) is classically expressed as a binary Bernoulli variable (event/no event) with a probability p_{it}:

$$y_{it} = \{0,1\} \sim B\{p_{it}\}. \quad \text{(Eq. 1)}$$

The time-space decomposition at the non-observable logit level is written as:

$$logit(p_{it}) = a_0 + POT_{it} + v_i + g_t + z_t, \quad \text{(Eq. 2)}$$

where a_o is a constant related to the overall mean activity, v_i is the spatial component of the signal—related to geomorphic variables, such as altitude, exposition, etc., acting on the activity of each path— $g_t + z_t$ is the detrended temporal anomaly—the sum of the long-term smoothed trend (g_t) with the year-to-year fluctuations (z_t)— and POT_{it} is the dendrogeomorphic potential, in other words the "potential" function that accounts for changes in the number of living trees in each path over the study period. The constraints $\sum_{i=1}^{N} v_i = 0$ and $\sum_{t=1}^{T} z_t = 0$ are set for identifiability purposes by construction (according to Eq. (10)) $\sum_{t=1}^{T} g_t = 0$.

We express the potential function as:

$$POT_{it} = a_{1i}\left(\frac{n_{it}}{n_{iT}}\right)^{a_{2i}}, \quad \text{(Eq. 3)}$$

where n_{it} is the number of living trees in a given path i a given year t in [1,T] and n_{iT} represents the maximum number of living trees in the specific path i, obtained for the final sampling year T over the period of record. a_{1i} and a_{2i} are two free parameters quantifying the strength and shape of the detrending in each path. Hence, the standardized potential noted *POTnorm* belongs to 0–1. It quantifying the capacity of the local tree stand to register avalanche activity in a given year and writes:

$$POTnorm_{it} = \frac{POT_{it}}{POT_{iT}} = \left(\frac{n_{it}}{n_{iT}}\right)^{a_{2i}}. \quad \text{(Eq. 4)}$$

Eventually, the detrended spatio-temporal avalanche activity is obtained while setting this standardized potential to 1. This leads, e.g., the detrended annual probability of avalanche occurrence in each path as:

$$p'_{it} = \frac{\exp(a_0 + a_{1i} + v_i + g_t + z_t)}{1 + \exp(a_0 + a_{1i} + v_i + g_t + z_t)}, \quad \text{(Eq. 5)}$$

and, by averaging over the different paths, the mean detrended annual probability of avalanche occurrence as:

$$p'_t = \frac{\exp\left(a_0 + \frac{1}{N}\sum_{i=1}^{N} a_{1i} + g_t + z_t\right)}{1 + \exp\left(a_0 + \frac{1}{N}\sum_{i=1}^{N} a_{1i} + g_t + z_t\right)}, \quad \text{(Eq. 6)}$$

or, alternatively, only the smooth component of the temporal signal as:

$$p'_{smooth_t} = \frac{\exp\left(a_0 + \frac{1}{N}\sum_{i=1}^{N} a_{1i} + g_t\right)}{1 + \exp\left(a_0 + \frac{1}{N}\sum_{i=1}^{N} a_{1i} + g_t\right)}. \quad \text{(Eq. 7)}$$

Symmetrically, the mean detrended spatial probability in each path is:

$$p'_i = \frac{\exp(a_0 + a_{1i} + v_i)}{1 + \exp(a_0 + a_{1i} + v_i)}. \quad \text{(Eq. 8)}$$

Eventually, the detrended mean inter-annual avalanche probability is simply:

$$p'_o = \frac{\exp\left(a_0 + \frac{1}{N}\sum_{i=1}^{N} a_{1i}\right)}{1 + \exp\left(a_0 + \frac{1}{N}\sum_{i=1}^{N} a_{1i}\right)}. \quad \text{(Eq. 9)}$$

The smoothed temporal trend is captured with the model proposed by Wahba (1978) who proposed an *a priori* distribution for the vector $g = (g_1, \ldots g_T)$ such that its Bayesian posterior expectation is a cubic smoothing spline. Speckman and Sun (2003) show that such a *priori* can be written as a 1-D intrinsic conditional autoregressive model (iCAR), where each value is the weighted mean of its neighbours, with improper density:

$$p\left(g \middle| \sigma_g^2, A\right) = \frac{|A|_+^{\frac{1}{2}}}{\sigma_g^{T-2}} \exp\left(\frac{-1}{2\sigma_g^2} g^{tr} A g\right), \quad \text{(Eq. 10)}$$

where A is a chosen semi-positive definite matrix with two null eigenvalues, and "||" and "*tr*"denote the matrix determinant and transpose operators. Here, we simply take A such that g is a second-order random walk, since Rue and Held (2005) showed that this approximation of Wahba (1978)'s *prior* leads to a smooth posterior mean. The variance-like parameter σ_g^2 controls the level of smoothing.

Eventually, classically, v_i and z_t are modelled as centred white noises, *i.e.*:

$$p\left(v_i \middle| \sigma_v^2\right) = \frac{1}{\sqrt{2\pi\sigma_v}} \exp\left(-\frac{v_i^2}{2\sigma_v^2}\right), \quad \text{(Eq. 11)}$$

$$p\left(z_t \middle| \sigma_z^2\right) = \frac{1}{\sqrt{2\pi\sigma_z}} \exp\left(-\frac{z_t^2}{2\sigma_z^2}\right). \quad \text{(Eq. 12)}$$

3.2.3. Variance decomposition

One important advantage of this model is that it allows easy quantification of the fraction of the total variability captured by the different terms. Indeed, the model's design makes all components independent. Hence, the total variance (*VAR*) at the logit layer is:

$$VAR(logit(p_{it})) = VAR(POT_{it}) + VAR(g_t) + \sigma_v^2 + \sigma_z^2, \quad \text{(Eq. 13)}$$

with $VAR(g_t)$ to be computed from the vector $g = (g_1, \ldots g_t)$ and $VAR(POT_{it})$ from the matrix POT_{it}.

By analogy to the classical R^2 adjustment statistics, the computation of variance ratios enables evaluation of the respective weight of the different terms in the modelled variability of avalanche occurrences:

$$R^2_{time\ trend} = \frac{VAR(g)}{VAR(logit(p_{it}))}, \quad \text{(Eq. 14)}$$

$$R^2_{time\ noise} = \frac{\sigma_z^2}{VAR(logit(p_{it}))}, \quad \text{(Eq. 15)}$$

$$R^2_{space} = \frac{\sigma_v^2}{VAR(logit(p_{it}))}, \quad \text{(Eq. 16)}$$

$$R^2_{POT} = \frac{VAR(POT_{it})}{VAR(logit(p_{it}))}, \quad \text{(Eq. 17)}$$

with the equality $R^2_{time\ trend} + R^2_{time\ noise} + R^2_{space} + R^2_{POT} = 1$.

Note that the specific weight of the detrending term in each path can be evaluated as:

$$R^2_{POT_i} = \frac{VAR(POT_{i.})}{VAR(POT_{i.}) + VAR(g_t) + \sigma^2_z}, \quad \text{(Eq. 18)}$$

where $VAR(POT_{i.})$ is the variance of the detrending term evaluated the considered path, only.

Eventually, the ratio:

$$R^2_{temp} = \frac{VAR(g_t)}{(VAR(g_t) + \sigma^2_z)}, \quad \text{(Eq. 19)}$$

is the classical signal-to-noise statistics within the temporal component.

3.2.4. Model inference and posterior estimates

The standard Bayesian Markov chain Monte Carlo method (MCMC; Gilks et al., 1995) allows to solve the inference challenge. Classical poorly informative *priors* were used, with the common assumption of *a priori* independence between the *prior* marginal distributions of each parameter. Robustness of the inference was checked on long simulation runs using tests based on starting different simulation runs at different points of the parameter space (Brooks and Gelman, 1998). The posterior distributions of all variance ratios were evaluated by computing their values at each point of the MCMC sequence.

In addition, we also evaluated the posterior distributions of different avalanche numbers to be confronted to the actual total number of reconstructed avalanches:

$$y_{tot_i} = \sum_{t=1}^{T} y_{it}, \quad \text{(Eq. 20)}$$

and

$$y_{tot} = \sum_{i=1}^{N} \sum_{t=1}^{T} y_{it}. \quad \text{(Eq. 21)}$$

These correspond to the number of snow avalanches which would have been reconstructed if there were no missing values in the chronologies, in each path *i* and in total, respectively. These missing years correspond, e.g., to the uneven length of the different tree-ring chronologies in the different paths.

In addition, sampling the predictive distribution $p'(y_{iT}) \sim dBern(p_{iT})$ lead estimates of the spatio-temporal homogenized avalanche activity, and, subsequently i) at the path scale over all the years or ii) over all the sets of sampled paths for each year, according to Eqs. (5)–(8). These detrended avalanche probabilities correspond to the avalanche frequencies that would have been reconstructed from tree rings if in each path the power of the tree-ring series to keep track of avalanche impacts would have been maximal all over the study period. Eventually, averaging over space and summing in time leads to an estimate y'_{tot} of the total homogenized avalanche number.

From all *posterior* distributions, we retained *posterior* means as point estimates and 95% credibility intervals to evaluate the corresponding uncertainty (Table 3).

Table 3
Number of reconstructed events per path according to their confidence level.

Slope	Path	Period	HCL	MCL	LCL	Total
Münster	MU 1	1726–2014	2	1	2	5
	MU 2	1751–2014	0	2	7	9
	MU 3	1720–2014	0	1	3	4
	MU 4	1768–2014	1	3	2	6
Geschinen	GE 1	1746–2014	4	3	16	23
	GE 2	1720–2014	1	1	15	17
Oberwald	OB 1	1720–2014	0	1	10	11
	OB 2	1720–2014	0	0	9	9
	OB 3	1720–2014	2	4	2	8
	OB 4	1720–2014	3	2	10	15
	OB 5	1738–2014	0	0	0	0
Total			**13**	**18**	**76**	**107**

3.3. Compilation of historical sources

The reliability of our detrended regional tree-ring reconstruction was tested by graphical comparison with a series of historical snow avalanche records from the Goms valley. To this end, we used several documentary sources to compile a precise and as complete as possible historical chronology of snow avalanches for Oberwald, Münster and Geschinen, with a specific focus on the studied paths, for the period 1720–2014.

First, we reviewed the annual winter report *Schnee und Lawinen in den Schweizer Alpen* from the Institute for Snow and Avalanche Research (WSL Institut für Schnee und Lawinenforschung SLF)—available since 1935, and annually since the 1950s (Laternser et al., 1997; Laternser and Schneebeli, 2002). This annual winter document reports all snow avalanches observed from SLF-observation stations spread over the Swiss Alps. Reported events are characterized by their triggering date—or, in the worst case, a period—and their location. Occasionally and unrelated to the snow avalanche intensity, additional information are available in the

Table 2
Intensity and types of growth disturbances (GD) identified in the 1014 sampled trees.

Type	Intensity	MU 1	MU 2	MU 3	MU 4	GE 1	GE 2	OB 1	OB 2	OB 3	OB 4	OB 5	Total
Injuries	very strong	4	1	9	8	14	10	8	12	9	18	8	101 (1.8%)
TRD, CT and CW	strong	15	13	28	16	82	85	58	71	45	57	46	516 (9.4%)
	medium	60	45	78	50	125	120	88	77	47	74	36	800 (14.5%)
	weak	129	114	192	132	331	287	270	211	60	125	65	1916 (34.8%)
GS	strong	19	8	21	14	26	22	30	29	27	48	29	273 (5.0%)
	medium	90	37	99	59	134	130	67	75	70	119	55	935 (17.0%)
	weak	29	16	56	32	92	116	176	110	73	191	70	961 (17.5%)
Total		**346 (6.3%)**	**234 (4.3%)**	**483 (8.8%)**	**311 (5.7%)**	**804 (14.6%)**	**770 (14.0%)**	**697 (12.7%)**	**585 (10.6%)**	**331 (6.0%)**	**632 (11.5%)**	**309 (5.6%)**	**5502 (100%)**

report's text such as deposit size, meteorological conditions or release area (Laternser and Schneebeli, 2002). For the same period, we complemented the series with information on snow avalanche expertly reported in technical reports (Stoffel et al., 2016a, 2016b).

Then, we examined a total of 8 local and regional newspapers published between 1841 and 2014—namely the Briger Anzeiger (1899–1960), Courrier du Valais (1843–1857, 1935–1938), Journal et Feuille d'Avis du Valais (1903–1968), Journal du Valais (1848, 1977–1978), Le Confédéré (1861–2009), Le Nouvelliste (1904–), Le Rhône (1929–1960), and Walliser Bote (1841–)—via the Swiss virtual newspaper archives available online at https://www.e-newspaperarchives.ch/. "Avalanche" and "Lawine" were the main keywords for the search and refer to the French and German words for snow avalanches. The names "Geschinen", "Münster" and "Oberwald" were used as keywords as they refer to the localities of the studied paths. In addition, "Bawald", "Bannwald", "Birchwald" and "Grimsle" were also used as keywords as they refer to the toponymy of the studied avalanche slopes.

In addition, we extracted the snow avalanche events compiled in the historical database of the *Forschungsinstitut zur Geschichte des Alpenraums* (FGA). This exceptional database contains a compilation of the main catastrophic events which took place in the Canton of Valais, before 1850, and which were related in ecclesiastical archives, stakeholder chronicles, administrative records, and legal archives. Eventually, duplicated events from the different databases were systematically removed, resulting in a single historical chronology.

3.4. Land cover changes

Forest cover changes evidence past destructive events but can also interfere, at decadal to centennial timescales, with avalanche activity (Zgheib et al., 2020). For the period 1881–2015, we documented the evolution of forest stands along the selected paths using historical series of cartographic documents (i.e., the Siegfried map, Obergesteln, 490, edition 1881 and aerial flight campaigns of 1946 and 2015 — available from the Federal Office of Topography, swisstopo; 1:20,000). All these documents manually digitized using ArcGIS 10.4 (ESRI, 2013; Kennedy, 2013) allowed quantification of forest cover evolution for 100-m elevation bands (Mainieri et al., 2020b).

We equally assessed forest dynamics at the path scale using the age structure of the stand. To this end, we counted the number of tree rings in each collected sample. In case the pith was absent, we estimated the number of missing rings using the "*Estimate Distance and Rings to Pith*" function of the Coo-Recorder 9.0 software (Larsson, 2016). During field campaigns, sampling positions ranged from 0.2 to 1.5 m above ground level. We used a branch whorl counting approach (Sorg et al., 2010; Van der Burght et al., 2012) as a correction factor to compensate for the time elapsed between germination and the moment a tree reaches sampling height. European larch *(Larix decidua* Mill.) is a typical heliophile pioneer species (Nardin et al., 2015) recolonizing surfaces cleared by snow avalanches or other mass movements to establish dominance within a few decades. The spatial analysis of the age distribution of larch trees has repeatedly been proven to help documentation of forest recolonization dynamics after destructive events (Stoffel et al., 2006; Van der Burght et al., 2012; Favillier et al., 2018). At the study site, mapping of the age structure at each stand was performed using an inverse distance weighted interpolation algorithm from individual tree ages using ArcGIS (IDW; ESRI, 2013; Kennedy, 2013).

4. Results

4.1. Age structure and land cover changes

In total, 525 (51.8%), 275 (27.1%) and 214 (21.1%) trees were sampled on the avalanche slopes of Oberwald, Geschinen and Münster (see Table 1). After cross-dating, sampled trees were, on average, 204 years old (SD ± 113 yrs, Table 1). The oldest and youngest trees were sampled in Geschinen (GE2) (Fig. 3a) and Oberwald (OB3) (Fig. 3c). They reached sampling height in 1336 and 1998 CE, respectively. At Münster and Oberwald, 100–300-yr old trees (68.0%) dominate the forest stands. By contrast, 0–100-year-old trees are scarce in the sampling distribution. Tree ages do not show specific spatial pattern that could suggest forest recolonization after a high-magnitude event. At GE1, the tree stand is younger and 57.8% of the sampled trees are less than 150 yrs old.

Sample size evolution (Fig. 3c) and the analysis of old maps suggest a continuous evolution of the forest stand (densification or rejuvenation) at Münster and Oberwald between 1720 and 1900; at Geschinen, the increasing number of sampled trees dated to 1890–1945 suggests a rapid colonization of the slope during this period. This evolution is confirmed by historical documents (Fig. 4). According to the Siegfried map (1881), the forest stands covered 102.1, 17.3, and 114.4 ha on the Münster (Fig. 4a), Geschinen (Fig. 4b) and Oberwald (Fig. 4c) avalanche slopes, respectively. Between 1881 and 2015, forest cover increased by 13.9 ha (+43%) in the MU release areas (1900–2100 m asl). Below 1800 m asl, forest colonization was more limited (+7.7 ha, +11%) and restricted to the main channels. Similarly, at OB, forest surfaces increased by 12.5 ha (+216%) and 10 ha (+25.0%) between 1500 and 1800 m asl, respectively. By contrast, in the GE paths, afforestation rates are significantly higher. The forest surface increased more than three times between 1881 (17.3 ha) and 2015 (58.8 ha) and extended by a factor of 13 (from 1.4 to 20.1 ha) above 1700 m asl, mainly in the release area (1800–2000 m asl) of snow avalanches.

4.2. Growth disturbances and snow avalanche activity

In total, we dated 5502 growth disturbances (GDs) in the tree-ring series—1511 at MU, 1650 at GE and 2764 at OB (Favillier et al., 2017). Table 2 summarizes the types and intensity of GDs at the path scale. Tangential rows of resin ducts (TRDs), callus tissue (CT) and compression wood (CW) were the most frequent (58.7%) GDs identified in the samples followed by growth suppression (GS; 39.4%). By contrast, only 101 injuries (I) were sampled. Weak (intensity 1) and intermediate intensity (2) reactions represented 52.3% and 31.5% of all GDs, respectively. Strong GDs and injuries, rated as intensities 3 and 4, represented 14.3% and 1.8% of all GDs, respectively. The oldest GD identified in the tree-ring series was dated back to 1383 CE. The annual frequency of GDs ranged between 0.027 (OB5) and 0.060 GD.yr^{-1} (GES1). On average, it increased from 0.014 GD.tree^{-1}.yr^{-1} (1720–1900) to 0.025 GD.tree^{-1}.yr^{-1} (1950–1979) to reach a maximum (0.029 GD.tree^{-1}.yr^{-1}) between 1980 and 2014. Injuries and GS are overrepresented in the GD spectrum before 1899 (Fig. 5). Conversely, during the 20th century, the latter is more homogeneous as the proportion of GD types is comparable over the periods 1900–1949 and 1980–2014 except for intense (strong-medium) TRD, CW and CT which are overrepresented between 1950 and 1979.

Based on the four-step procedure, GDs allowed identification of 107 snow avalanche events occurring in 73 different avalanche years between 1720 and 2014 in the 11 paths (Fig. 6, Table 3). Synchronous avalanche events occurred in at least two paths in 23 out of the 73 avalanche years. Moreover, synchronous avalanche events were reconstructed in at least 3 paths in 8 avalanche years,

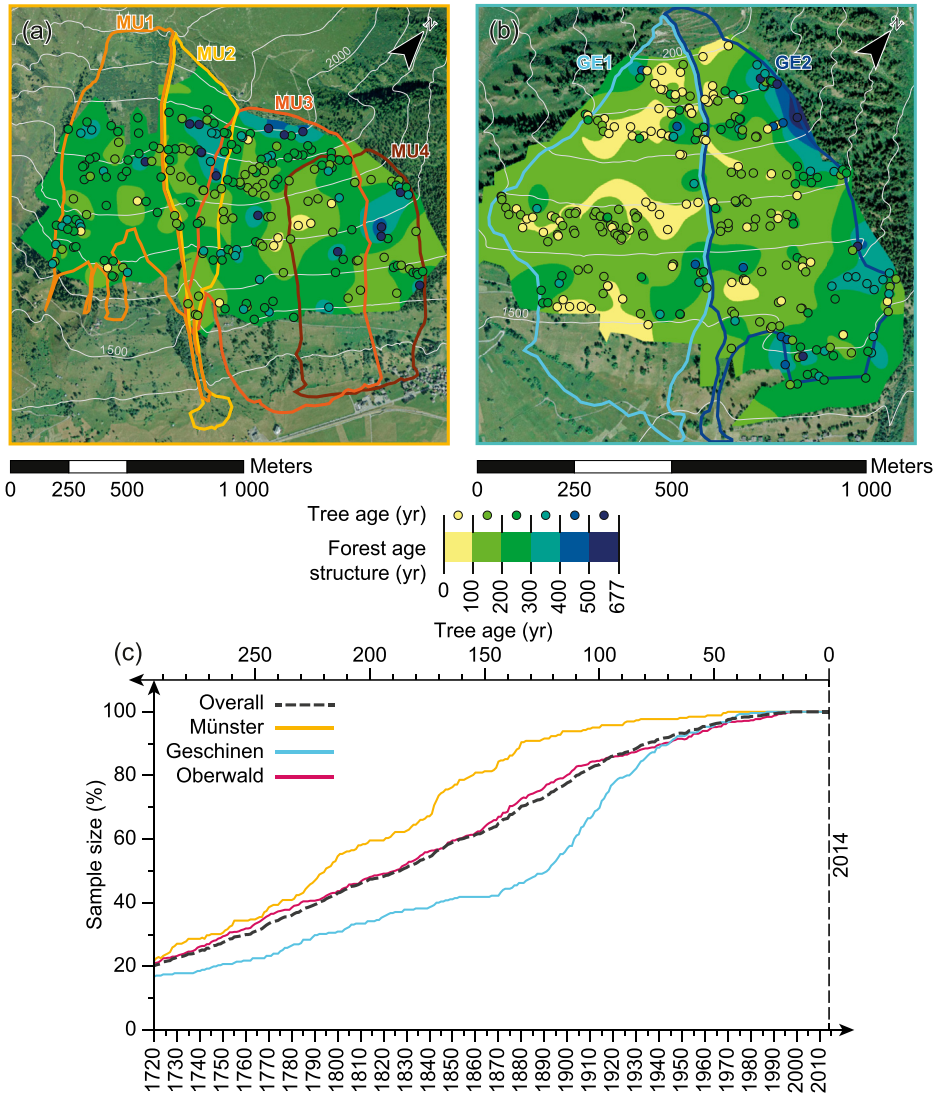

Fig. 3. Age structure of the forest stands growing in the Goms valley: spatial distribution of individual trees sampled and interpolated tree ages at (a) Münster and (b) Geschinen; (c) evolution the sample size on the three avalanche slopes. The black dashed line represents the overall sample size evolution. Age structure maps and the spatial distribution of sampled trees at Oberwald are shown in Favillier et al. (2017).

namely in 1795 (3), 1945 (3), 1982 (3), 1983 (3), 1990 (4), 1996 (3), 2002 (4) and 2003 (4). The oldest (1772) and the most recent events (2014) occurred at path GE2. In total, the procedure allowed reconstruction of 43 snow avalanches (40.2%) at OB (5 paths), 24 (22.4%) at MU (4 paths) and 40 (37.4%) at GE (2 paths). At the path scale, GE1 and GE2 had the most significant snow avalanche activity with 23 events between 1795 and 2009 and 17 events between 1772 and 2013, respectively. By contrast, 0, 5 (1794–2012), 4 (1911–1994) and 6 events (1834–2006) were retrieved at OB5, MU1, MU3 and MU4, respectively.

At step 2 of the procedure, comparisons also highlighted 90 potential avalanche events that coincide with larch budmoth outbreak episodes or extreme climatic years. Amongst these potential events, we excluded 60 from the reconstruction and considered 30 with a low level of confidence (LLC). At step 3, we rated 13 and 18 events with high (HLC) and medium (MLC) level of confidence, respectively. By comparison, 76 events with a weighted It index W_{it}<0.2 —characterized by a majority of weak and medium GDs — were reconstructed with a LLC (Table 3). Events rated with high and medium levels of confidence mainly occurred at GE1 (4 HLC, 3 MLC) OB4 (3 HLC, 4 MLC), and OB3 (2 HLC, 4 MCL). By contrast, we attributed low levels of confidence to most reconstructed events at GE2 (15 LLC), OB1 (10 LLC), OB2 (9 LLC), and MU2 (7 LLC).

The correlation matrix (Fig. 7) computed between path reconstructions over the period 1768–2014 — for which sample size ≥60% — showed highest correlations between MU3 and MU4 ($r > 0.6$; $\alpha < 0.001$). Lower ($r \approx 0.2$), albeit significant, correlations were also computed between OB2-OB3-OB4 and GE1-GE2. By contrast, correlations computed between paths from different slopes were not statistically significant, thus demonstrating asynchronous variations of avalanche activity.

4.3. Comparison with historical chronicles

Analysis of historical sources yielded data on 23 avalanche events in 19 years in the 11 studied paths between 1720 and 2014 (Fig. 8). Multiple snow avalanches occurred within the studied paths during winters 1720 (2; GE, OB), 1945 (2; GE, MU), 1951 (2; GE, OB) and 1999 (2; MU, OB). In total, 5 (26%) of the 19 avalanche

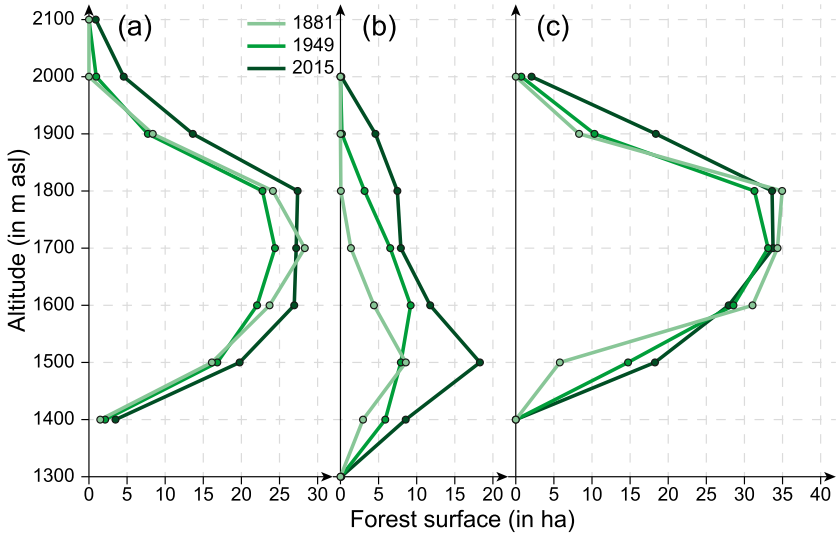

Fig. 4. Evolution of the forest cover (1881–2015) as a function of elevation at (a) Münster, (b) Geschinen and (c) Oberwald.

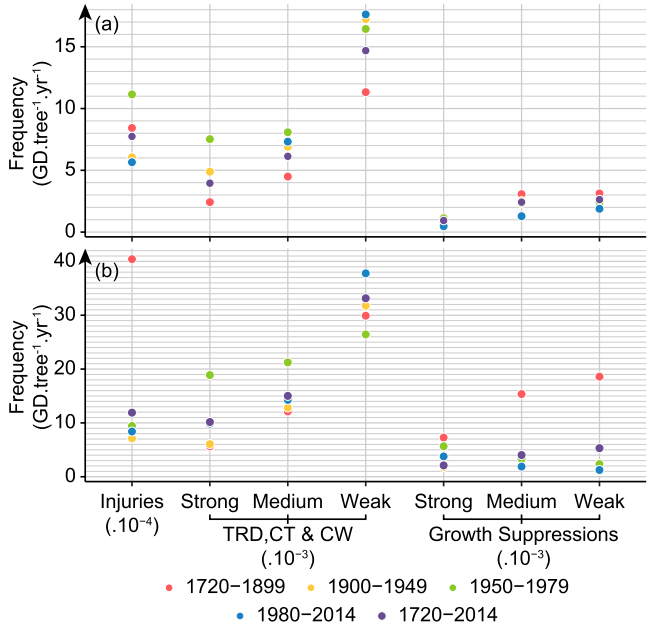

Fig. 5. Distributions of growth disturbance (GD) types and intensities between 1720 and 2014. We only include GDs that could be attributed clearly to snow avalanches and thus excludes anomalies induced by insect outbreaks and/or extreme climatic conditions. Panel (a) contains all GDs attributed to reconstructed avalanche event. Panel (b) includes all GDs present in the ring series. The y-axis has been scaled and expanded by GD type and intensity. GD frequencies are given in GD tree^{-1} yr^{-1} $\times$ 10^{-4} for injuries and GD tree^{-1} yr^{-1} $\times$ 10^{-3} for TRD, CT, CW and GS.

years retrieved from the site-specific historical chronicles were also reconstructed with tree-ring records, namely in 1935 (OB2), 1945 (GE), 1966 (OB), 1999 (0B3) and 2003 (OB3). An insufficient number of GDs and/or possible interferences with larch budmoth outbreaks, climatic extremes (cold summer or drought) and limitations inherent to dendrogeomorphic reconstructions did not permit retrieval of the other events. For example, although historical archives reported snow avalanches in 1951 at OB1, OB3 and GE1, these events were visible in several tree-ring samples but neither in sufficient number nor with sufficiently intense reactions to be retrieved with sufficient confidence as events in the tree-ring series. Also, they did not affect the age structure of the stand.

The historical database reports 218 avalanche events (77 avalanche years, Fig. 8a) in the Goms valley between 1720 and 2014. Tree-ring analysis realized in Geschinen, Münster and Oberwald allowed reconstruction of 35 out of the 77 avalanche years (45%) found in historical archives; in addition, tree-ring and historical records share 180 common years in which no avalanche event was reported. Pearson's Chi-squared test suggests that both time series are significantly correlated ($\alpha < 0.05$). The historical database reveals major avalanche winters in 1896 (25 events), 1951 (13), 1967 (9), 1978 (8) and 1999 (29) (Fig. 8). Amongst these winters, tree-ring analysis allowed reconstructed of snow avalanches in 1978 and 1999 with 1 (GE2) and 2 events (OB3, OB4), respectively (Figs. 6 and 8b). Conversely, years with two or more reconstructed event years in our tree-ring derived chronology—1911, 1928, 1945, 1953, 1971, 1982, 1983, 1990, 1996 and 2002–2003—did not appear as exceptional in historical archives.

4.4. Hierarchical modelling of snow avalanche activity at the regional scale

The Bayesian hierarchical model described in Section 3.2 has been used to homogenise the regional snow avalanche reconstruction between 1766 and 2014 (Fig. 9). As the first snow avalanche reconstructed in the chronology occurred in 1772 (GE2) and to optimize the modelling process, we considered $t_0 = 1766$ as the starting date for the homogenized regional chronology, which corresponds to the year of the oldest detected event minus the mean recurrence interval between consecutive snow avalanches for the period 1772–1900. Global parameters of the model (Table 4) indicate that the variations of the dendrogeomorphic potential (POT, related to decreasing sample size back in time) explains 28% of the variability of the spatio-temporal variability of snow avalanche activity as reconstructed by tree rings (the 11 raw chronologies). The smoothed (decadal) temporal trend (g_t, Eq. (14)) and the year-to-year fluctuations (z_t, Eq. (15)) of avalanche activity represent 61% and 4% of the modelled variability, respectively—the smooth term representing 93% of the common temporal variability. Finally, the spatial component v_i only explains 7% of the total variance.

In total, the Bayesian hierarchical model estimates that almost

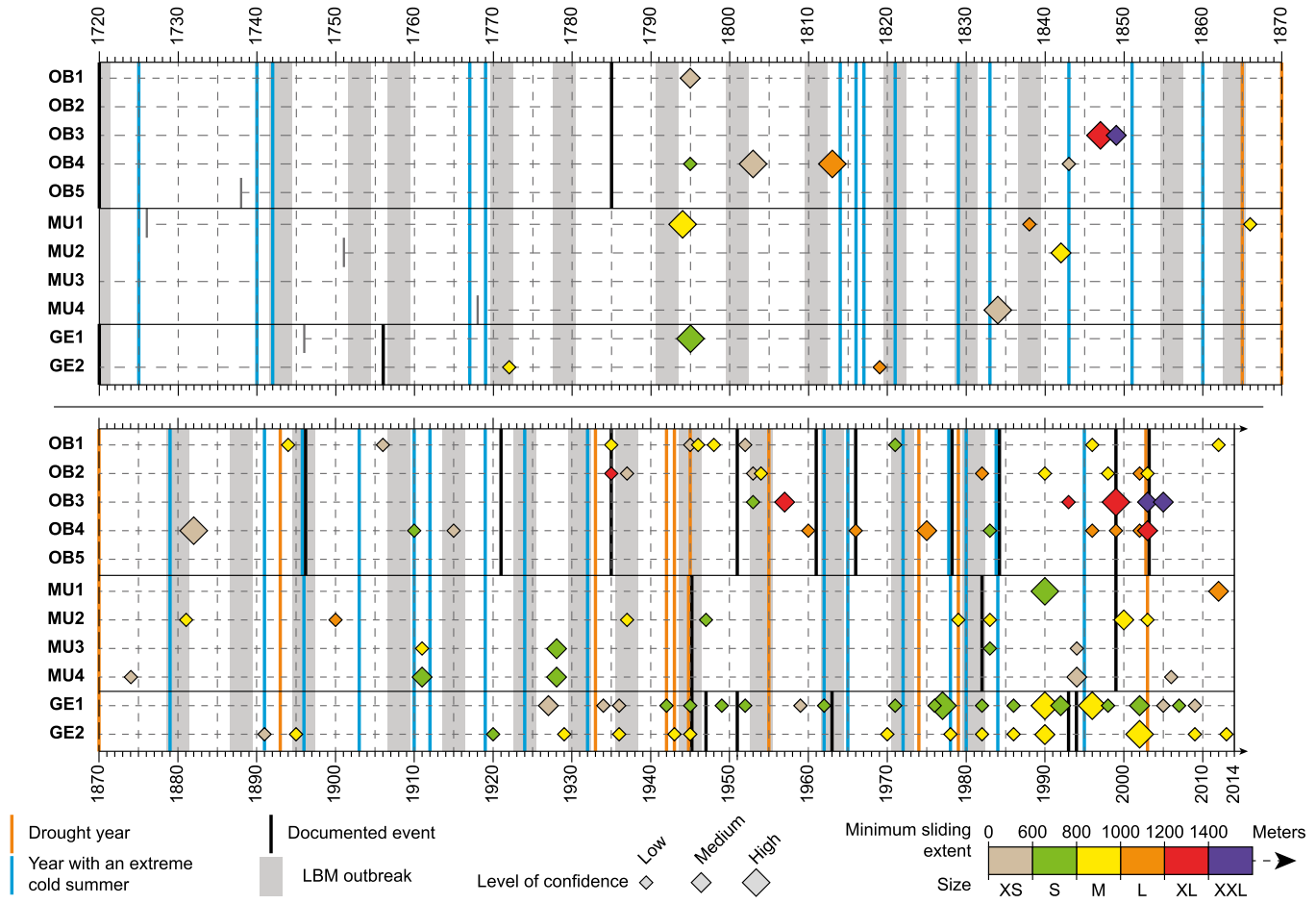

Fig. 6. Avalanche events reconstructed for the period 1720–2014 in the 11 avalanche paths based on the 4-step procedure (Favillier et al., 2017). Symbol sizes are proportional to the level of confidence. The colour range highlights the minimum slide extent as derived from the position of impacted trees. Grey bands represent triplets of years associated to larch budmoth (LBM) outbreaks. Vertical lines show snow avalanche events documented in site-specific historical chronicles (black), as well as extremely dry (orange) and cold (blue) summers.

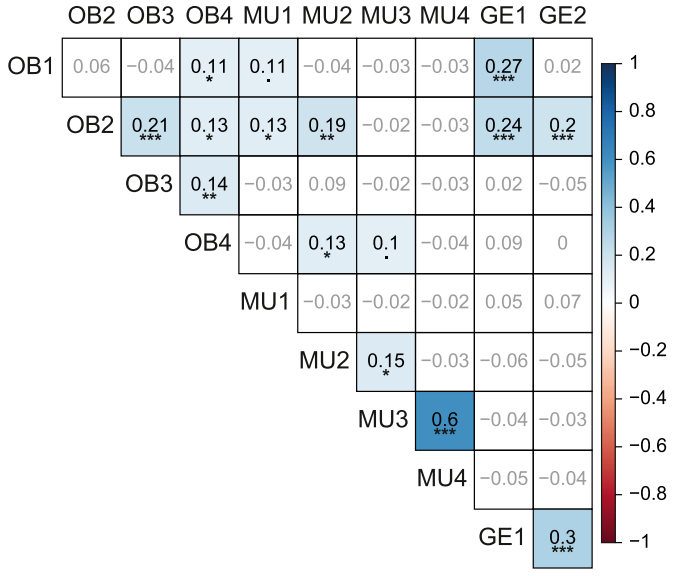

Fig. 7. Comparison of raw snow avalanche activity at the path scale for the period 1720–2014. Non-significant correlation coefficients – according to the Student test are shown in grey. Significance levels are rated by a. ($\alpha = 0{,}1$), * ($\alpha = 0{,}05$), ** ($\alpha = 0{,}01$), *** ($\alpha = 0{,}001$).

no events were missed in the regional chronology due to the insufficient length of MU4 reconstruction (y_{tot} is estimated equal to 107, namely the actual reconstructed number of avalanches). This is logical since only two years are missing and in one single path only. In addition, the model estimates that $y'_{tot} = 139$ [90–206] snow avalanches would have been retrieved from tree rings over the 1766–2014 period with a constant maximal tree-ring potential (i.e., +30% with respect to the activity that could be retrieved from tree rings). This corresponds to a mean annual homogenized snow avalanche probability p'_0 of 0.026 (Eq. (9)), or one avalanche per path every 38 years on average.

In terms of the estimated dendrogeomorphic potential (POT, Eq. (3), Supplementary Table S1), the highest multiplicative correction factor (a_1) is found in path GE1 (3.8) where the standardized POT increased strongly over time from 0.16 in 1766 to 1 in 1987 (1). The POT multiplicative correction factor also exceeds a value of 2 at GE2 (2.6), OB2 (2.4), OB4 (2.4) and OB3 (2.0), highlighting significant increase over time in the capacity of trees to keep memory of past avalanches in their tree rings. By contrast, the lowest a_1 values are found at MU1 (0.96) and MU3 (1.1), pointing to an almost constant dendrogeomorphic potential in these paths over time. The shape correction factor (a_2) strongly departs from 1.7 in OB2 and is estimated to 0.48 in OB4. In all other paths, it is rather close to 1. This explains the overall linear shape of the mean dendrogeomorphic

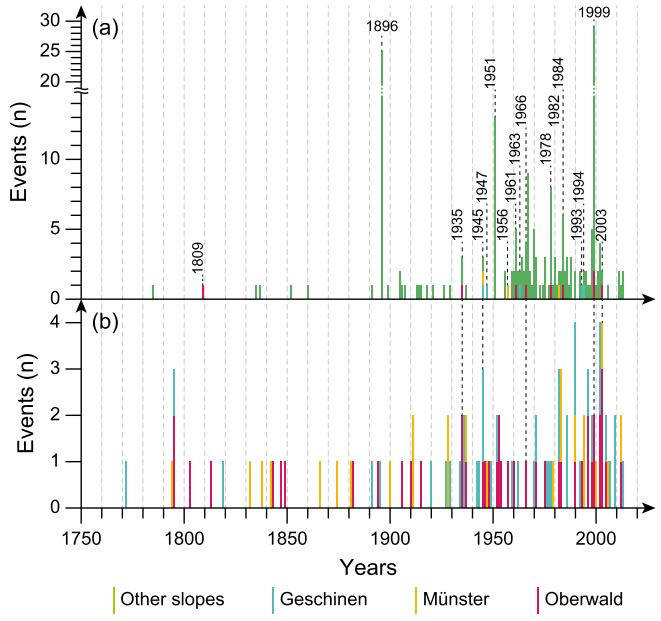

Fig. 8. Comparison of (a) past avalanches in the Goms valley recorded in historical records with (b) tree-ring reconstructed snow avalanches. Green bars represent the annual number of snow avalanches recorded in the historical database. Blue, orange, and pink bars indicate the annual number of snow avalanches in Geschinen, Münster and Oberwald, respectively. Black dashed lines highlight events where matches are found between dendrogeomorphic and historical records.

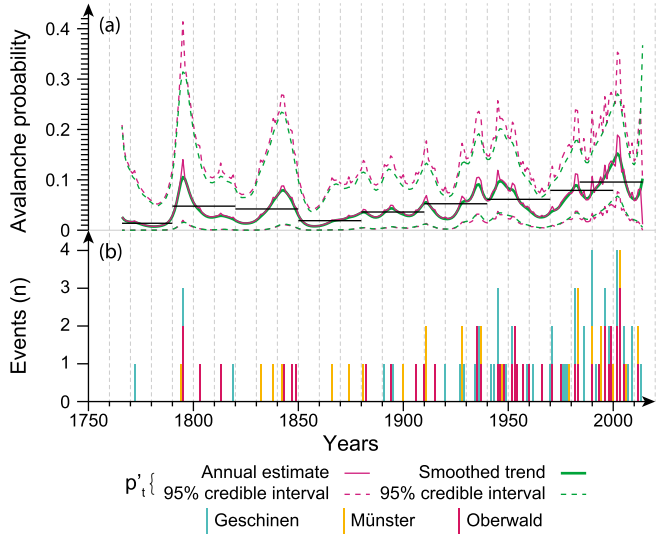

Fig. 9. (a) Homogenized regional snow avalanche activity derived from the dendrogeomorphic reconstruction using a Hierarchical Bayesian Modelling approach. Violet and green lines represent annual and decadal snow avalanche probabilities provided by the model. Dashed lines indicate the 95% confidence level. The horizontal black lines represent the mean probability of snow avalanches computed from 30-yr periods (empirical mean of model estimates). (b) Raw chronology of reconstructed snow avalanche events with blue, orange, and purple bars for the Geschinen, Münster and Oberwald slopes, respectively.

potential, and the faster increase at the beginning/end of the study period at Münster and Geschinen, respectively (Fig. 10).

From a spatial perspective, detrended results show higher local mean interannual snow avalanche probabilities (Eq. (8)) at GE1 (0.12 events.year^{-1}, [confidence interval: 0.05–0.24]), GE2 (0.05 events.year^{-1}, [0.02–0.11[), OB4 (0.04 events.year^{-1}, [0.2–0.09])

Table 4
Posterior characteristics of the Hierarchical Bayesian Model parameters. For each parameter, the posterior average, and the lower and upper bounds of the 95% credible interval were extracted.

	Mean	***2.5%***	***97.5%***
σ_g	0.37	0.03	1.66
σ_v	0.35	0.25	0.51
σ_z	0.23	0.18	0.28
$R^2_{time\ trend}$ (Eq. (14))	0.61	0.2	0.87
$R^2_{time\ noise}$ (Eq. (15))	0.04	0.01	0.09
R^2_{space} (Eq. (16))	0.07	0	0.38
R^2_{POT} (Eq. (17))	0.28	0.09	0.52
R^2_{temp} (Eq. (19))	0.93	0.84	0.98
y'_{tot}	139.2	90	206

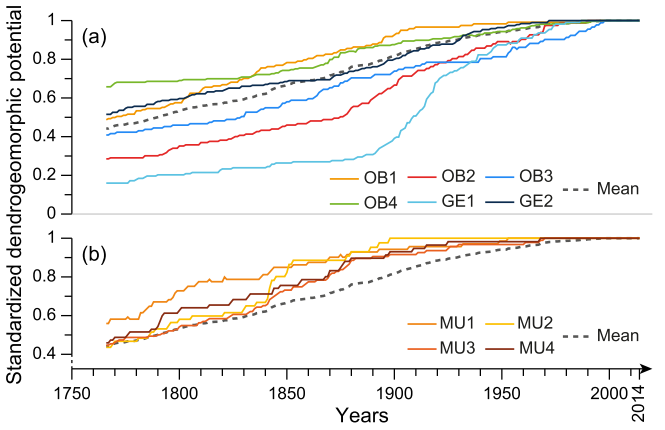

Fig. 10. Evolution over the study period of the standardized dendrogeomorphic potential (POTnorm) as estimated by the model at (a) Oberwald, Geschinen and b) Münster. In a-b), the grey dashed line indicates the mean evolution of the standardized dendrogeomorphic potential over the 11 paths.

and OB2 (0.04 events.year^{-1}, [0.01–0.09]). At MU1 (0.010 events.year^{-1}, [0.00–0.02]), MU3 (0.010 events.year^{-1}, [0.00–0.03]) and MU4 (0.014 events.year^{-1}, [0.02–0.10]), these homogenized mean interannual probabilities are significantly lower.

The maximum homogenized annual probability of avalanches (Eq. (6)) occurred in 2002 (p' = 0.19 events.year^{-1}), 2003 (0.18), 1795 (0.14), 1999 (0.14), and 2000 (0.13) (Fig. 9). By contrast, the probability was 20 times smaller in 1781 (0.0076), 1782 (0.0077), 1780 (0.0078), 1783 (0.0081), and 1857 (0.0082). At the decadal scale, p'$_{smooth}$ (Eq. (7)) increased between 1996 and 2005 (0.13), 1944–1953 (0.9), and 1792–1801 (0.08); it was significantly lower for 1777–1786 (p'$_{smooth}$ = 0.008), 1854–1863 (0.009), and 1820–1829 (0.015). Over the period 1766–2014, the 30-yr homogenized snow avalanche probability (Fig. 9) reached a first maximum in 1790–1819 (0.048 event.yr^{-1}) and 1820–1849 (0.042) to continuously increase since the end of the 19th century, from 0.036 (1880–1909) to 0.096 event.yr^{-1} (1985–2014). According to the Mann-Kendall test, this trend is statistically significant ($\leq$0.001). Yet, uncertainties were, on average, 0.13 for the period 1766–2014, with minimum and maximum widths for the 95% confidence intervals observed between 1854 and 1863 (0.08) and 1792–1801 (0.25), respectively. At the centennial timescale, the 95% confidence interval width increased between the 19th century (1801–1900: 0.11) and 1901–2014 (0.14).

5. Discussion

In this study, we reconstructed avalanche activity in 11

avalanche paths in the Goms valley (Swiss Alps) using growth disturbances dated in 1014 trees affected by snow avalanches to document 107 snow avalanches in 73 different years between 1720 and 2014. This exceptionally long and dense dataset was then used to build a "regional" chronology, with the aim of obtaining real changes in avalanche activity in the region. Despite the unusually dense dataset, we find considerable variation in avalanche activity between the different paths and a weak synchronism in activity in adjacent paths. One might therefore wonder what the best scale would be to detect a common signal that reflects a significant regional evolution in avalanche activity related to large-scale climate change and/or socio environmental drivers rather than peculiarities of the chosen sample of paths. So far, definitions on which scale/path number is best suited to this aim is missing. Relying on a very dense dataset of past snow avalanches from a large set of ~3000 avalanche paths in the French Alps, Eckert et al. (2013) evidenced that averaging the record over a large number of paths will be mostly free from local artefacts and thus provides a large-scale signal that is possibly linked to climate variability and change. Yet, their study also showed that the overall temporal pattern inferred was relatively weak, as it mixed contrasted north/south evolutions related to interactions between regional climate change and topography of mountain massifs. The authors therefore recommended the use of their approach to smaller subregions with potentially more homogeneous avalanche activity, so as to infer the most significant response of avalanche activity to climate change or other large-scale drivers — yet this has not been done so far and was therefore applied to the Goms valley in this study.

5.1. Challenging reconstruction of avalanche activity at the regional scale

To do so, we employed an updated model-based Hierarchical Bayesian Modelling (HBM) approach (Eckert et al., 2007, 2010; Lavigne et al., 2012; Giacona et al., 2021) to account for the specificities of tree-ring reconstructions and especially decreasing sample depth back in time. A HBM approach allows extraction of trends and significant patterns underlying snow avalanche activity (such as change-points), with different sources of uncertainty treated rigorously by taking missing values and uncertainty regarding annual estimates into account when inferring temporal patterns of interest. The main advantages and limitations of this framework for the analysis and interpretation of multiple series of mass movement records have been discussed extensively (e.g., Jomelli et al., 2015). A major benefit of this approach is that it respects the binary structure of data and thereby eliminates the need of arbitrary thresholds to identify active/inactive years/paths in regional reconstructions. In addition, the framework allows for a full decomposition of space and time effects in occurrence probabilities, thereby revealing potential climatic trend shared by all years/paths, and a clear distinction of such from residual random effects. Hence, it allows linkage of large-scale trends with local effects in a fair and consistent way (Eckert and Giacona, 2022). The HBM framework presented here is therefore much more flexible than those used in existing studies (Decaulne et al., 2012, 2014; Germain et al., 2009; Martin and Germain, 2017; Voiculescu et al., 2016; Peitzsch et al., 2021a, 2021b) where fluctuations of avalanche activity at the regional scale were simply related to the percentage of injured trees in a given year. By contrast to the regional avalanche activity index approach—in which some paths can be more influential (Peitzsch et al., 2021a)—the HBM framework thus prevents overemphasizing any local reconstruction in the homogenized chronology. An additional strength of HBM comes from the consideration of correlations between sites and years, which allows accounting for sites where data is lacking.

Specifically, our HBM includes a term specifically designed to remove potential trends in tree-ring based avalanche chronologies resulting from a decreasing number of living trees back in time to precisely quantify the number of missed events and to homogenise snow avalanche activity at the regional level. The added value of such an approach was previously demonstrated for avalanche occurrence data from historical sources (Giacona et al., 2021). In our case, the model suggests that the percentage of missed events is limited (30%) such that differences between the raw and homogenized regional chronologies are small. As the model was formulated independent of the study case, we argue that it could even be more useful in cases for which the percentage of missed events is much higher than in our case (i.e., regions with scarce information on ancient avalanche activity).

The HBM framework also allows independent distinction of the spatial (v_i) and temporal ($g_t + z_t$) components and the definition of variance ratios expressing the respective weight of different terms in modelled variability in snow avalanche probabilities. We reveal that the temporal term explains a considerably larger part of total variability of reconstructed avalanche activity (64.8%) when compared to the spatial term (7.3%), indicating that the common variables changing over time (e.g., climatic, or other large scale environmental trends) play a key important role in controlling avalanche activity in the Goms valley. By contrast, the impacts of steady local conditions explaining the variability of the p'_i of individual paths—such as path morphometry—are much less significant in explaining the spatio-temporal variability in process activity. This also suggests that the number of paths included in the Goms valley reconstruction, albeit higher than that of most published dendrogeomorphic studies, remains insufficient to properly reproduce variability in avalanche activity at the regional scale. The fact that only 7% of the total variability is explained by steady local conditions is arguably too low; this value should be considerably higher as shown in large inventories of systematic records of several thousands of paths in the French Alp (Eckert et al., 2010; Lavigne et al., 2015).

From a temporal perspective, decadal and interannual fluctuations in avalanche activity shared a high proportion of variance in the homogenized reconstruction. This points to a predominant control of snow avalanching by large-scale environmental variables that evolve consistently over time. Yet, the fraction of temporal variability explained by the smooth trend may be too strong with regards to reality (i.e., year-to-year variability as function of natural variability in winter conditions). It may be attributable to the well-known shrinkage effect of HBM models, in which model estimates tends to favor smooth robust trends rather than departures from trends when information quantity is low (e.g., Wikle, 2003; Eckert et al., 2013). Another complimentary explanation is the underestimation of the real inter-path variability related to their variable topography, activity, or forest stand. This results from too small a number of paths, i.e. the inferred temporal signal is biased towards the common behaviour of the 11 paths studied without capturing the full regional variability.

Indeed, the main advantage of the HBM framework over classic aggregation methods used in dendrogeomorphic reconstructions is that it represents a rigorously derived mean snow avalanche signal for a given region. Yet, and given the limited set of couloirs used in this study, we cannot affirm that the signal found is really representative for the entire region. In other words, one might ask whether the selection of a similar number of adjacent couloirs would have yielded the same results. Also, we realize that 11 couloirs may not have been a large enough sample — at least in the case of this region — to obtain a robust signal. We therefore see a need for even larger regional reconstructions relying on the model presented in this study (or other similar models) so as to better

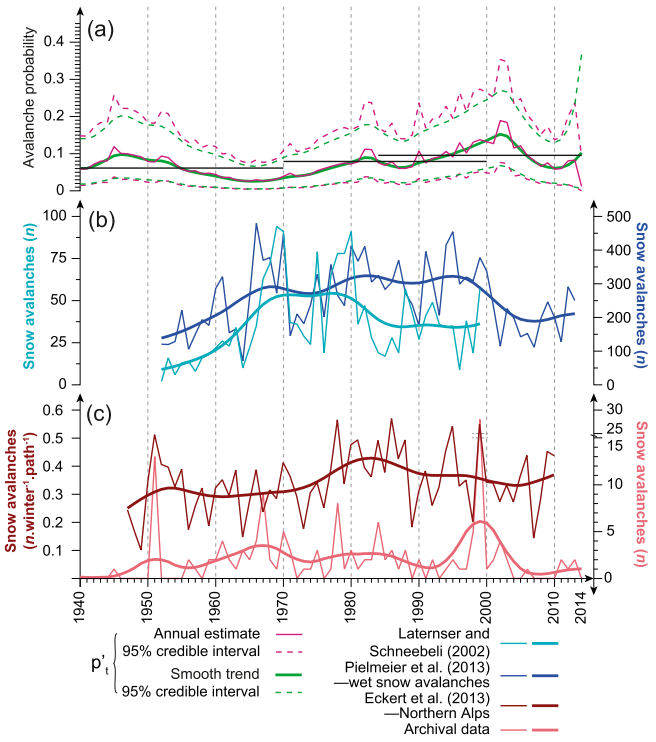

Fig. 11. Comparison between (a) the regional avalanche activity inferred in this study and (b) other avalanche activity indicators for the Swiss (Laternser and Schneebeli, 2002; Pielmeier et al., 2013) (c) and French (Eckert et al., 2013) Alps. In (a), the violet and green lines represent annual and decadal snow avalanche probabilities, dashed lines indicate the 95% confidence level. The horizontal black lines represent the mean probability of snow avalanche computed for 30-yr periods (empirical mean of annual estimates). In (b) and (c), the thin coloured lines represent interannual activity and the bold line represents decadal activity computed as the average of annual estimates on a 11-yr period.

define the minimum number of couloirs needed and the criteria to select these couloirs (i.e., in terms of activity, forest stand density) to produce a temporal signal that becomes invariant over a given geographical area.

5.2. Temporal avalanche signal in tree-ring reconstructions and historical record

In the homogenized reconstruction, annual avalanche probabilities peaked over the 1790–1800s and 1840–1850s, in addition, an increasing trend was observed over the 20th century, reaching a maximum between 2005 and 2014. Despite the stringency of the approach developed here—both in terms of the detection of past events and the extraction of a common regional signal—we only find limited agreement with historical archives for the Goms valley and/or snow avalanche records covering the Swiss and French Alps (Fig. 11). At the annual scale, the rate of agreement between the dendrogeomorphic avalanche chronology and archival data (26%) is significantly lower than those reported in previous studies in the French Alps by Corona et al. (2012, 43%), Corona et al. (2013, 43%), Schläppy et al. (2013, 38%), Schläppy et al. (2014, 33–45%) or de Bouchard d'Aubeterre et al. (2019, >70%). This limited convergence could result from limitations of path-scale tree-ring reconstructions discussed extensively in the literature (Corona et al., 2012). For instance, snow avalanches of insufficient magnitude to impact trees or major avalanches that destroyed large parts of the forest stand and may remove evidence of past and subsequent events or disturb tree growth in such a way that younger events cannot be identified in the tree-ring record (Favillier et al., 2018).

Fluctuations in the modelled smoothed trend (g_t) in avalanche activity (Fig. 11a) are poorly in line with other alpine studies: Eckert et al. (2013) (Fig. 11c), for instance, highlighted a slight decrease in avalanche activity in systematic inventories in the French Alps during the 1960s, whereas Schneebeli et al. (1997; Fig. 11b), Laternser and Schneebeli (2002), Eckert et al. (2013) and Pielmeier et al. (2013) failed to detect a significant trend in the number of winters with low/high activity in the French and Swiss Alps since the 1990s. Eventually, we did not find any decrease in overall avalanche activity over the last decades and therefore cannot confirm a possible role of higher temperatures and scarcer snow conditions (Eckert et al., 2013; Giacona et al., 2021; Peitzsch et al., 2021b) at our sites. Even if a status-quo or an increase in avalanche activity cannot be ruled out at the paths investigated due to the elevation of the release areas (Lavigne et al., 2015), the absence of any trend since the 1990s is surprising as (i) important efforts have been undertaken over the course of the 20th century to install countermeasures designed to limit avalanche activity in a majority of the paths, especially after the Second World War, (ii) an increase and a densification of the forest cover in the upper part of the avalanche couloirs at MU, OB and especially GE has been documented since the end of the 19th century. This limited convergence at decadal timescales between our "regional" reconstruction, large-scale historical records from the Goms valley and known drivers of changes in avalanche activity (i.e. climate warming, systematic construction of defence structures) may have various, maybe even combined origins: lacunar historical sources, an overrepresentation of extreme snow avalanches in tree-ring reconstructions resulting in a temporal signal that is biased with regards to true process activity, or, again, too small a set of couloirs considered in the tree-ring reconstruction not allowing the detection of a truly representative regional signal.

6. Conclusions

The Hierarchical Bayesian modelling framework used in this study allows rigorous extraction of a mean common snow avalanche signal of different couloirs as it takes account of local artefacts, forest dynamics, sample size evolutions and potentially missing events as well as non-stationarities, all of which up to now precluded consistent as well as spatially and temporally stable assessments of past process activity with dendrogeomorphic techniques. Yet, despite the stringency of the approach, the homogenized regional avalanche chronology shows poor convergence with avalanche chronicles existing for the Goms valley as well as for the Swiss and French Alps. The limited convergence between different data sources has multiple reasons. First of all, whereas dendrogeomorphic approaches were limited to 11 avalanche paths, the archival records are from all avalanche-producing sites in the region. In addition, regional datasets built from archival records will have a tendency to contain primarily extreme events that led to human losses and infrastructural damage, whereas tree-ring based reconstruction tend to yield data on intermediate magnitude which are of sufficient size and intensity to damage trees without destroying the forest stand. Last but not least, the limited synchronicity also raises questions regarding couloir selection and the number of couloirs to be considered in tree-ring reconstructions that aim at capturing a regional evolution related to large-scale drivers rather than to the peculiarities of the chosen path sample. Although we included 11 paths—a number that exceeds a large majority of previously published studies— we realize that the sample size was still too small to capture the variability of avalanche occurrences in both space and time. Future studies employing the HBM framework should investigate much

larger datasets to define the minimum number of couloirs needed for the reconstructed regional avalanche signal to become independent from the sites selected. In addition, we advocate for future work to focus more on trends rather than on the activity in individual years for which different paths may exhibit differing process behaviours. By doing so, dendrogeomorphic records will complement information from historical records, especially for smaller- and intermediate-magnitude snow avalanches which are critically missing in archives (Giacona et al., 2017; 2021).

Authors contributions

Adrien Favillier: Conceptualization, Methodology, Formal analysis, Writing — original draft; **Sébastien Guillet**: Fieldwork, Resources; **Jérôme Lopez-Saez**: Resources, Writing — review & editing; **Florie Giacona**: Resources, Writing — review & editing; **Nicolas Eckert**: Conceptualization, Methodology, Supervision, Resources, Formal analysis, Writing — original draft, review, editing; **Gregor Zenhäusern**: Resources; **Jean-Luc Peiry**: Supervision, Funding acquisition; **Markus Stoffel**: Conceptualization, Supervision, Resources, Funding acquisition, Writing — review & editing; **Christophe Corona**: Conceptualization, Methodology, Formal analysis, Funding acquisition, Writing — original draft, review, editing.

Declaration of competing interest

The authors declare that they have no known competing financial interests or personal relationships that could have appeared to influence the work reported in this paper.

Data availability

The authors are unable or have chosen not to specify which data has been used.

Acknowledgements

IGE/INRAE is member of Labex OSUG. Finally, the authors acknowledge Erich H. Peitzsch and one anonymous reviewers for their helpful and very positive comments on the manuscript and to Donatella Magri for the thorough editing.

Appendix A. Supplementary data

Supplementary data to this article can be found online at https://doi.org/10.1016/j.quascirev.2023.108063.

References

Alestalo, J., 1971. Dendrochronological interpretation of geomorphic processes. Fennia 105, 1–139.
Arbellay, E., Stoffel, M., Decaulne, A., 2013. Dating of snow avalanches by means of wound-induced vessel anomalies in sub-arctic Betula pubescens. Boreas 42, 568–574. https://doi.org/10.1111/j.1502-3885.2012.00302.x.
Ballesteros-Cánovas, J.A., Trappmann, D., Madrigal-González, J., Eckert, E., Stoffel, M., 2018. Climate warming enhances snow avalanche risk in the Western Himalayas. Proc. Natl. Acad. Sci. U.S.A. 13, 3410–3415. https://doi.org/10.1073/pnas.1716913115.
Battipaglia, G., Frank, D., Büntgen, U., Dobrovolnỳ, P., Brázdil, R., Pfister, C., Esper, J., 2010. Five centuries of Central European temperature extremes reconstructed from tree-ring density and documentary evidence. Global Planet. Change 72, 182–191.
Bollati, I., Crosa Lenz, B., Golzio, A., Masseroli, A., 2018. Tree rings as ecological indicator of geomorphic activity in geoheritage studies. Ecol. Indicat. 93, 899–916. https://doi.org/10.1016/j.ecolind.2018.05.053.
Bollschweiler, M., Stoffel, M., Schneuwly, D.M., 2008. Dynamics in debris-flow activity on a forested cone — a case study using different dendroecological approaches. Catena 72, 67–78. https://doi.org/10.1016/j.catena.2007.04.004.
Boucher, D., Filion, L., Hétu, B., 2003. Reconstitution dendrochronologique et fréquence des grosses avalanches de neige dans un couloir subalpin du mont Hog's Back, en Gaspésie centrale (Québec). Géogr. Phys. Quaternaire 57, 159–168. https://doi.org/10.7202/011311ar.
Brooks, S.P., Gelman, A., 1998. General methods for monitoring convergence of iterative simulations. J. Comput. Graph Stat. 7, 434–455. https://doi.org/10.1080/10618600.1998.10474787.
Bryant, C.L., Butler, D.R., Vitek, J.D., 1989. A statistical analysis of tree-ring dating in conjunction with snow avalanches: comparison of on-path versus off-path responses. Environ. Geol. Water Sci. 14, 53–59. https://doi.org/10.1007/BF01740585.
Büntgen, U., Frank, D., Liebhold, A., Johnson, D., Carrer, M., Urbinati, C., Grabner, M., Nicolussi, K., Levanic, T., Esper, J., 2009. Three centuries of insect outbreaks across the European Alps. New Phytol. 182, 929–941. https://doi.org/10.1111/j.1469-8137.2009.02825.x.
Butler, D.R., 1979. Snow avalanche path terrain and vegetation, glacier national park, Montana. Arct. Alp. Res. 11, 17–32. https://doi.org/10.2307/1550456.
Butler, D.R., 1987. Teaching general principles and applications of dendrogeomorphology. J. Geol. Educ. 35, 64–70. https://doi.org/10.5408/0022-1368-35.2.64.
Butler, D.R., Malanson, G.P., 1985. A Reconstruction of Snow-Avalanche Characteristics in Montana, U.S.A., Using Vegetative Indicators. J. Glaciol. 31, 185–187. https://doi.org/10.3189/S0022143000006444.
Butler, D.R., Sawyer, C.F., 2008. Dendrogeomorphology and high-magnitude snow avalanches: a review and case study. Nat. Hazards Earth Syst. Sci. 8, 303–309. https://doi.org/10.5194/nhess-8-303-2008.
Carrara, P.E., 1979. The determination of snow avalanche frequency through tree-ring analysis and historical records at Ophir, Colorado. Geol. Soc. Am. Bull. 90, 773–780. https://doi.org/10.1130/0016-7606(1979)90<773:TDOSAF>2.0.CO;2.
2007 Casteller, A., Stöckli, V., Villalba, R., Mayer, A.C., 2007. An Evaluation of Dendroecological Indicators of Snow Avalanches in the Swiss Alps, 218:AEODIO Arctic Antarct. Alpine Res. 39 (39), 218–228. https://doi.org/10.1657/1523-0430, 2.0.CO;2.
Casteller, A., Christen, M., Villalba, R., Martínez, H., Stöckli, V., Leiva, J.C., Bartelt, P., 2008. Validating numerical simulations of snow avalanches using dendrochronology: the Cerro Ventana event in Northern Patagonia, Argentina. Nat. Hazards Earth Syst. Sci. 8, 433–443. https://doi.org/10.5194/nhess-8-433-2008.
Casteller, A., Villalba, R., Araneo, D., Stöckli, V., 2011. Reconstructing temporal patterns of snow avalanches at Lago del Desierto,southern Patagonian Andes. Cold Reg. Sci. Technol. 67, 68–78. https://doi.org/10.1016/j.coldregions.2011.02.001.
Casteller, A., Häfelfinger, T., Cortés Donoso, E., Podvin, K., Kulakowski, D., Bebi, P., 2018. Assessing the interaction between mountain forests and natural hazards at Nevados de Chillán, Chile, and its implications for Ecosystem-based Disaster Risk Reduction. Nat. Hazards Earth Syst. Sci. 1173–1186. https://doi.org/10.5194/nhess-18-1173-2018.
Chiroiu, P., Stoffel, M., Onaca, A., Urdea, P., 2015. Testing dendrogeomorphic approaches and thresholds to reconstruct snow avalanche activity in the Făgăraş Mountains (Romanian Carpathians). Quat. Geochronol. 27, 1–10. https://doi.org/10.1016/j.quageo.2014.11.001.
Coaz, J., 1910. Statistik und Verbau der Lawinen in den Schweizeralpen. Im Auftrag des eidgenössischen Departementes des Innern, Stämpfli, Bern.
Corona, C., Rovéra, G., Lopez Saez, J., Stoffel, M., Perfettini, P., 2010. Spatio-temporal reconstruction of snow avalanche activity using tree rings: Pierres Jean Jeanne avalanche talus, Massif de l'Oisans, France. Catena 83, 107–118. https://doi.org/10.1016/j.catena.2010.08.004.
Corona, C., Lopez Saez, J., Stoffel, M., Bonnefoy, M., Didier, R., Astrade, L., Berger, F., 2012. How much the real avalanche activity can be captured with tree rings? An evaluation of classic dendrogeomorphic approaches and comparison with historical archives. Cold Reg. Sci. Technol. 74 (75), 31–42. https://doi.org/10.1016/j.coldregions.2012.01.003.
Corona, C., Lopez Saez, J., Stoffel, M., Rovéra, G., Edouard, J.-L., Berger, F., 2013. Seven centuries of avalanche activity at Echalp (Queyras massif, southern French Alps) as inferred from tree rings. Holocene 23, 292–304. https://doi.org/10.1177/0959683612460784.
Cressie, N., Wikle, C.K., 2011. Statistics for Spatio-Temporal Data. John Wiley & Sons.
de, G., Favillier, A., Mainieri, R., Lopez Saez, J., Eckert, N., Saulnier, M., Peiry, J.-L., Stoffel, M., Corona, C., 2019. Tree-ring reconstruction of snow avalanche activity: Does avalanche path selection matter? Sci. Total Environ. 684, 496–508. https://doi.org/10.1016/j.scitotenv.2019.05.194.
Decaulne, A., Eggertsson, Ó., Sæmundsson, Þ., 2012. A first dendrogeomorphologic approach of snow avalanche magnitude–frequency in Northern Iceland. Geomorphology 167–168, 35–44. https://doi.org/10.1016/j.geomorph.2011.11.017.
Decaulne, A., Eggertsson, Ó., Laute, K., Beylich, A.A., 2014. A 100-year extreme snow-avalanche record based on tree-ring research in upper Bødalen, inner Nordfjord, western Norway. Geomorphology 218, 3–15. https://doi.org/10.1016/j.geomorph.2013.12.036.

Dubé, S., Filion, L., Hétu, B., 2004. Tree-Ring Reconstruction of High-Magnitude Snow Avalanches in the Northern Gaspé Peninsula, Québec, Canada. Arctic Antarct. Alpine Res. 36, 555–564.
Eckert, N., Giacona, F., 2022. Towards a holistic paradigm for long-term snow avalanche risk assessment and mitigation. Ambio. https://doi.org/10.1007/s13280-022-01804-1.
Eckert, N., Parent, E., Belanger, L., Garcia, S., 2007. Hierarchical Bayesian modelling for spatial analysis of the number of avalanche occurrences at the scale of the township. Cold Reg. Sci. Technol. 50, 97–112. https://doi.org/10.1016/j.coldregions.2007.01.008.
Eckert, N., Parent, E., Kies, R., Baya, H., 2010. A spatio-temporal modelling framework for assessing the fluctuations of avalanche occurrence resulting from climate change: application to 60 years of data in the northern French Alps. Clim. Change 101, 515–553. https://doi.org/10.1007/s10584-009-9718-8.
Eckert, N., Keylock, C.J., Castebrunet, H., Lavigne, A., Naaim, M., 2013. Temporal trends in avalanche activity in the French Alps and subregions: from occurrences and runout altitudes to unsteady return periods. J. Glaciol. 59, 93–114. https://doi.org/10.3189/2013JoG12J091.
Efthymiadis, D., Jones, P.D., Briffa, K.R., Auer, I., Böhm, R., Schöner, W., Frei, C., Schmidli, J., 2006. Construction of a 10-min-gridded precipitation data set for the Greater Alpine Region for 1800–2003. J. Geophys. Res. 111. https://doi.org/10.1029/2005JD006120.
Esper, J., Buntgen, U., Frank, D.C., Nievergelt, D., Liebhold, A., 2007. 1200 years of regular outbreaks in alpine insects. Proc. R. Soc. B Biol. Sci. 274, 671–679. https://doi.org/10.1098/rspb.2006.0191.
ESRI, 2013. ArcGIS 10.2.1. Redlands, CA.
Favillier, A., Guillet, S., Morel, P., Corona, C., Lopez-Saez, J., Eckert, N., Ballesteros Cánovas, J.A., Peiry, J.-L., Stoffel, M., 2017. Disentangling the impacts of exogenous disturbances on forest stands to assess multi-centennial tree-ring reconstructions of avalanche activity in the upper Goms Valley (Canton of Valais, Switzerland). Quat. Geochronol. 42, 89–104. https://doi.org/10.1016/j.quageo.2017.09.001.
Favillier, A., Guillet, S., Trappmann, D., Morel, P., Lopez-Saez, J., Eckert, N., Zenhäusern, G., Peiry, J.-L., Stoffel, M., Corona, C., 2018. Spatio-temporal maps of past avalanche events derived from tree-ring analysis: A case study in the Zermatt valley (Valais, Switzerland). Cold Reg. Sci. Technol. 154, 9–22. https://doi.org/10.1016/j.coldregions.2018.06.004.
Gądek, B., Kaczka, R.J., Rączkowska, Z., Rojan, E., Casteller, A., Bebi, P., 2017. Snow avalanche activity in Żleb Żandarmerii in a time of climate change (Tatra Mts., Poland). Catena 158, 201–212. https://doi.org/10.1016/j.catena.2017.07.005.
Garavaglia, V., Pelfini, M., 2011. The role of border areas for dendrochronological investigations on catastrophic snow avalanches: A case study from the Italian Alps. Catena 87, 209–215. https://doi.org/10.1016/j.catena.2011.06.006.
Germain, D., 2016. A statistical framework for tree-ring reconstruction of high-magnitude mass movements: case study of snow avalanches in eastern canada. Geogr. Ann. Ser. Phys. Geogr. 98, 303–311. https://doi.org/10.1111/geoa.12138.
Germain, D., Filion, L., Hétu, B., 2005. Snow avalanche activity after fire and logging disturbances, northern Gaspé Peninsula, Quebec, Canada. Can. J. Earth Sci. 42, 2103–2116. https://doi.org/10.1139/e05-087.
Germain, D., Filion, L., Hétu, B., 2009. Snow avalanche regime and climatic conditions in the Chic-Choc Range, eastern Canada. Clim. Change 92, 141–167. https://doi.org/10.1007/s10584-008-9439-4.
Germain, D., Pop, O.T., Gratton, M., Holobâcă, I.-H., Burada, C., 2022. Snow-avalanche hazard assessment based on dendrogeomorphic reconstructions and classification tree algorithms for ski area development, Parâng Mountains, Romania. Cold Reg. Sci. Technol. 201, 103612. https://doi.org/10.1016/j.coldregions.2022.103612.
Giacona, F., Eckert, N., Corona, C., Mainieri, R., Morin, S., Stoffel, M., Martin, B., Naaim, M., 2021. Upslope migration of snow avalanches in a warming climate. Proc. Natl. Acad. Sci. USA 118, e2107306118. https://doi.org/10.1073/pnas.2107306118.
Gilks, W.R., Richardson, S., Spiegelhalter, D., Richardson, S., Spiegelhalter, D., 1995. Markov Chain Monte Carlo in Practice. Chapman and Hall/CRC. https://doi.org/10.1201/b14835.
Gratton, M., Germain, D., Boucher, É., 2019. Meteorological triggering scenarios of tree-ring-based snow avalanche occurrence on scree slopes in a maritime climate, Eastern Canada. Phys. Geogr. 1–18. https://doi.org/10.1080/02723646.2019.1573622.
Hebertson, E.G., Jenkins, M.J., 2003. Historic climate factors associated with major avalanche years on the Wasatch Plateau, Utah. Cold Reg. Sci. Technol. 37, 315–332. https://doi.org/10.1016/S0165–232X(03)00073-9.
Ives, J.D., Mears, A.I., Carrara, P.E., Bovis, M.J., 1976. Natural Hazards in Mountain Colorado. Ann. Assoc. Am. Geogr. 66, 129–144. https://doi.org/10.1111/j.1467-8306.1976.tb01076.x.
Jenkins, M.J., Hebertson, E.G., 2004. A practitioner's guide for using dendroecological techniques to determine the extent and frequency of avalanches. Proc. 2004 Int. Snow Sci. Workshop 423–434.
Johnson, A.L., Smith, D.J., 2010. Geomorphology of snow avalanche impact landforms in the southern Canadian Cordillera: Geomorphology of snow avalanche impact landforms. Can. Geogr. 54, 87–103. https://doi.org/10.1111/j.1541-0064.2009.00275.x.
Jomelli, V., Pavlova, I., Eckert, N., Grancher, D., Brunstein, D., 2015. A new hierarchical Bayesian approach to analyse environmental and climatic influences on debris flow occurrence. Geomorphology 250, 407–421. https://doi.org/10.1016/j.geomorph.2015.05.022.
2004 Kajimoto, T., Daimaru, H., Okamoto, T., Otani, T., Onodera, H., 2004. Effects of Snow Avalanche Disturbance on Regeneration of Subalpine Abies mariesii Forest, Northern Japan, 0436:EOSADO Arctic Antarct. Alpine Res. 36 (36), 436–445. https://doi.org/10.1657/1523-0430, 2.0.CO;2.
Kennedy, M., 2013. Introducing Geographic Information Systems with ArcGIS: a Workbook Approach to Learning GIS, third ed. John Wiley & Sons, Hoboken, New Jersey.
Kogelnig-Mayer, B., Stoffel, M., Schneuwly-Bollschweiler, M., Hübl, J., Rudolf-Miklau, F., 2011. Possibilities and Limitations of Dendrogeomorphic Time-Series Reconstructions on Sites Influenced by Debris Flows and Frequent Snow Avalanche Activity. Arctic Antarct. Alpine Res. 43, 649–658. https://doi.org/10.1657/1938-4246-43.4.649.
Kogelnig-Mayer, B., Stoffel, M., Schneuwly-Bollschweiler, M., 2013. Four-dimensional growth response of mature Larix decidua to stem burial under natural conditions. Trees (Berl.) 27, 1217–1223. https://doi.org/10.1007/s00468-013-0870-4.
Köse, N., Aydın, A., Akkemik, Ü., Yurtseven, H., Güner, T., 2010. Using tree-ring signals and numerical model to identify the snow avalanche tracks in Kastamonu, Turkey. Nat. Hazards 54, 435–449. https://doi.org/10.1007/s11069-009-9477-x.
Krause, D., Křížek, M., 2018. Dating of recent avalanche events in the Eastern High Sudetes, Czech Republic. Quat. Int. A 166. https://doi.org/10.1016/j.quaint.2017.09.001. –175.
Larocque, S.J., Hétu, B., Filion, L., 2001. Geomorphic and dendroecological impacts of slushflows in central gaspé peninsula (québec, canada). Geogr. Ann. Ser. Phys. Geogr. 83, 191–201. https://doi.org/10.1111/j.0435-3676.2001.00154.x.
Larsson, L.-Å., 2016. CDendro & CooRecorder Program Package for Tree Ring Measurements and Crossdating of the Data, Version 8.1.1. Cybis Elektronik & Data AB, Saltsjöbaden, Sweden.
Laternser, M., Schneebeli, M., 2002. Temporal trend and spatial distribution of avalanche activity during the last 50 years in Switzerland. Nat. Hazards 27, 201–230.
Laternser, M., Pfister, C., 1997. Avalanches in Switzerland 1500-1990. In: Frenzel, B., Matthews, J., Gläser, A., Weiss, M. (Eds.), Rapide Mass Movement since the Holocene, pp. 241–266.
Lavigne, A., Bel, L., Parent, E., Eckert, N., 2012. A model for spatio-temporal clustering using multinomial probit regression: application to avalanche counts. Environmetrics 23, 522–534. https://doi.org/10.1002/env.2167.
Lavigne, A., Eckert, N., Bel, L., Parent, E., 2015. Adding expert contributions to the spatiotemporal modelling of avalanche activity under different climatic influences. J. R. Stat. Soc. Ser. C Appl. Stat. 64, 651–671. https://doi.org/10.1111/rssc.12095.
Laxton, S.C., Smith, D.J., 2009. Dendrochronological reconstruction of snow avalanche activity in the Lahul Himalaya, Northern India. Nat. Hazards 49, 459–467. https://doi.org/10.1007/s11069-008-9288-5.
Lempa, M., Kaczka, R.J., Rączkowska, Z., Janecka, K., 2016. Combining tree-ring dating and geomorphological analyses in the reconstruction of spatial patterns of the runout zone of snow avalanches, Rybi Potok Valley, Tatra Mountains (Poland). Geogr. Pol. 89, 31–45. https://doi.org/10.7163/GPol.004.
Lopez Saez, J., Corona, C., Stoffel, M., Gotteland, A., Berger, F., Liébault, F., 2011. Debris-flow activity in abandoned channels of the Manival torrent reconstructed with LiDAR and tree-ring data. Nat. Hazards Earth Syst. Sci. 11, 1247–1257. https://doi.org/10.5194/nhess-11-1247-2011.
Lopez Saez, J., Corona, C., Stoffel, M., Astrade, L., Berger, F., Malet, J.-P., 2012. Dendrogeomorphic reconstruction of past landslide reactivation with seasonal precision: the Bois Noir landslide, southeast French Alps. Landslides 9, 189–203. https://doi.org/10.1007/s10346-011-0284-6.
Mainieri, R., Corona, C., Chartoire, J., Eckert, N., Lopez-Saez, J., Stoffel, M., Bourrier, F., 2020a. Dating of rockfall damage in trees yields insights into meteorological triggers of process activity in the French Alps. Earth Surf. Process. Landf. n/a. https://doi.org/10.1002/esp.4876.
Mainieri, R., Favillier, A., Lopez Saez, J., Eckert, N., Zgheib, T., Morel, P., Saulnier, Mélanie, Peiry, J.-L., Stoffel, M., Corona, C., 2020b. Impacts of land-cover changes on snow avalanche activity in the French Alps. Anthropocene 13. https://doi.org/10.1016/j.ancene.2020.100244.
Malik, I., Wistuba, M., Migoń, P., Fajer, M., 2016. Activity of Slow-Moving Landslides Recorded in Eccentric Tree Rings of Norway Spruce Trees (Picea Abies Karst.) — An Example from the Kamienne MTS. (Sudetes MTS., Central Europe). Geochronometria 43. https://doi.org/10.1515/geochr-2015-0028.
Martin, J.-P., Germain, D., 2016a. Can we discriminate snow avalanches from other disturbances using the spatial patterns of tree-ring response? Case studies from the Presidential Range, White Mountains, New Hampshire, United States. Dendrochronologia 37, 17–32. https://doi.org/10.1016/j.dendro.2015.12.004.

Martin, J.-P., Germain, D., 2016b. Dendrogeomorphic reconstruction of snow avalanche regime and triggering weather conditions A classification tree model approach. Prog. Phys. Geogr. 40, 0309133315625863. https://doi.org/10.1177/0309133315625863.
Martin, J.-P., Germain, D., 2017. Large-scale teleconnection patterns and synoptic climatology of major snow-avalanche winters in the Presidential Range (New Hampshire, USA). Int. J. Climatol. 37, 109–123. https://doi.org/10.1002/joc.4985.
Meseșan, F., Gavrilă, I.G., Pop, O.T., 2018a. Calculating snow-avalanche return period from tree-ring data. Nat. Hazards. https://doi.org/10.1007/s11069-018-3457-y.
Meseșan, F., Man, T.C., Pop, O.T., Gavrilă, I.G., 2018b. Reconstructing snow avalanche extent using remote sensing and dendrogeomorphology in Parâng Mountains. Cold Reg. Sci. Technol. https://doi.org/10.1016/j.coldregions.2018.10.002.
Mundo, I.A., Barrera, M.D., Roig, F.A., 2007. Testing the utility of Nothofagus pumilio for dating a snow avalanche in Tierra del Fuego, Argentina. Dendrochronologia 25, 19–28. https://doi.org/10.1016/j.dendro.2007.01.001.
Muntán, E., Andreu, L., Oller, P., Gutiérrez, E., Martínez, P., 2004. Dendrochronological study of the Canal del Roc Roig avalanche path: first results of the Aludex project in the Pyrenees. Ann. Glaciol. 38, 173–179. https://doi.org/10.3189/172756404781815077.
Muntán, E., García, C., Oller, P., Martí, G., García, A., Gutiérrez, E., 2009. Reconstructing snow avalanches in the Southeastern Pyrenees. Nat. Hazards Earth Syst. Sci. 9, 1599–1612. https://doi.org/10.5194/nhess-9-1599-2009.
Nardin, M., Musch, B., Rousselle, Y., Guérin, V., Sanchez, L., Rossi, J.-P., Gerber, S., Marin, S., Pâques, L.E., Rozenberg, P., 2015. Genetic differentiation of European larch along an altitudinal gradient in the French Alps. Ann. For. Sci. 72, 517–527. https://doi.org/10.1007/s13595-015-0483-8.
Oven, D., Levanič, T., Jež, J., Kobal, M., 2019. Reconstruction of Landslide Activity Using Dendrogeomorphological Analysis in the Karavanke Mountains in NW Slovenia. Forests 10, 1009. https://doi.org/10.3390/f10111009.
Pederson, G.T., Reardon, B.A., Caruso, C.J., Fagre, D.B., 2006. High Resolution Tree-Ring Based Spatial Reconstructions of Snow Avalanche Activity in Glacier National Park, Montana, USA. Presented at the Internation Snow Science Workshop, Telluride, Colorado, USA, pp. 436–443.
Peitzsch, E.H., Hendrikx, J., Stahle, D., Pederson, G., Birkeland, K., Fagre, D., 2021a. A regional spatiotemporal analysis of large magnitude snow avalanches using tree rings. Nat. Hazards Earth Syst. Sci. 21, 533–557. https://doi.org/10.5194/nhess-21-533-2021.
Peitzsch, E.H., Pederson, G.T., Birkeland, K.W., Hendrikx, J., Fagre, D.B., 2021b. Climate drivers of large magnitude snow avalanche years in the U.S. northern Rocky Mountains. Sci. Rep. 11, 10032. https://doi.org/10.1038/s41598-021-89547-z.
Pielmeier, C., Techel, F., Marty, C., Stucki, T., 2013. Wet snow avalanche activity in the Swiss Alps - trend analysis for mid-winter season. Proc. Int. Snow Sci. Workshop 1240–1246.
Pop, O.T., Gavrilă, I.-G., Roșian, G., Meseșan, F., Decaulne, A., Holobâcă, I.H., Anghel, T., 2016. A century-long snow avalanche chronology reconstructed from tree-rings in Parâng Mountains (Southern Carpathians, Romania). Quat. Int. 415, 230–240. https://doi.org/10.1016/j.quaint.2015.11.058.
Pop, O.T., Munteanu, A., Flaviu, M., Gavrilă, I.-G., Timofte, C., Holobâcă, I.-H., 2017. Tree-ring-based reconstruction of high-magnitude snow avalanches in Piatra Craiului Mountains (Southern Carpathians, Romania). Geogr. Ann. Ser. Phys. Geogr. 1–17. https://doi.org/10.1080/04353676.2017.1405715.
Potter, N., 1969. Tree-Ring Dating of Snow Avalanche Tracks and the Geomorphic Activity of Avalanches, Northern Absaroka Mountains, Wyoming. Geol. Soc. Am. Spec. Pap. 123, 141–166. https://doi.org/10.1130/SPE123-p141.
Püntener, C., Stoffel, M., Schneuwly-Bollschweiler, M., 2012. Frequenz und Fliesshöhen der Plattlaui (Uri), rekonstruiert mithilfe von Jahrringen. Schweiz. Z. Forstwes. 163, 445–450. https://doi.org/10.3188/szf.2012.0445.
Rayback, S.A., 1998. A dendrogeomorphological analysis of snow avalanche in the Colorado Front Range, USA. Phys. Geogr. 19, 502–515. https://doi.org/10.1080/02723646.1998.10642664.
Reardon, B.A., Pederson, G.T., Caruso, C.J., Fagre, D.B., 2008. Spatial Reconstructions and Comparisons of Historic Snow Avalanche Frequency and Extent Using Tree Rings in Glacier National Park, Montana, U.S.A. Arct. Antarct. Alp. Res. 40, 148–160. https://doi.org/10.1657/1523-0430(06-069 [REARDON]2.0.CO;2.
Rue, H., Held, L., 2005. Gaussian Markov Random Fields: Theory and Applications. Chapman and Hall/CRC. https://doi.org/10.1201/9780203492024.
Schaerer, P.A., 1972. In: Slaymaker, O., McPherson, H.J. (Eds.), Terrain and Vegetation of Snow Avalanche Sites at Rogers Pass, British Columbia in Mountain Geomorphology. Mountain Geomorphology: Geomorphological Processes in the Canadian Cordillera, Vancouver B.C., pp. 215–222
Schläppy, R., Jomelli, V., Grancher, D., Stoffel, M., Corona, C., Brunstein, D., Eckert, N., Deschatres, M., 2013. A New Tree-Ring-Based, Semi-Quantitative Approach for the Determination of Snow Avalanche Events: use of Classification Trees for Validation. Arctic Antarct. Alpine Res. 45, 383–395. https://doi.org/10.1657/1938-4246-45.3.383.
Schläppy, R., Eckert, N., Jomelli, V., Stoffel, M., Grancher, D., Brunstein, D., Naaim, M., Deschatres, M., 2014. Validation of extreme snow avalanches and related return periods derived from a statistical-dynamical model using tree-ring techniques. Cold Reg. Sci. Technol. 99, 12–26. https://doi.org/10.1016/j.coldregions.2013.12.001.
Schläppy, R., Jomelli, V., Eckert, N., Stoffel, M., Grancher, D., Brunstein, D., Corona, C., Deschatres, M., 2016. Can we infer avalanche–climate relations using tree-ring data? Case studies in the French Alps. Reg. Environ. Change 16, 629–642. https://doi.org/10.1007/s10113-015-0823-0.
Schneebeli, M., Laternser, M., Walter, A., 1997. Destructive snow avalanches and climate change in the Swiss Alps. Eclogae Geol. Helv. 457–461.
Schneuwly, D.M., Stoffel, M., Bollschweiler, M., 2009a. Formation and spread of callus tissue and tangential rows of resin ducts in Larix decidua and Picea abies following rockfall impacts. Tree Physiol. 29, 281–289. https://doi.org/10.1093/treephys/tpn026.
Schneuwly, D.M., Stoffel, M., Dorren, L.K.A., Berger, F., 2009b. Three-dimensional analysis of the anatomical growth response of European conifers to mechanical disturbance. Tree Physiol. 29, 1247–1257. https://doi.org/10.1093/treephys/tpp056.
Shroder, J.F., 1980. Dendrogeomorphology: review and new techniques of tree-ring dating. Prog. Phys. Geogr. 4, 161–188. https://doi.org/10.1177/030913338000400202.
Šilhán, K., Stoffel, M., 2015. Impacts of age-dependent tree sensitivity and dating approaches on dendrogeomorphic time series of landslides. Geomorphology 236, 34–43. https://doi.org/10.1016/j.geomorph.2015.02.003.
Šilhán, K., Tichavský, R., 2017. Snow avalanche and debris flow activity in the High Tatras Mountains: New data from using dendrogeomorphic survey. Cold Reg. Sci. Technol. 134, 45–53. https://doi.org/10.1016/j.coldregions.2016.12.002.
Šilhán, K., Kluzová, O., Tichavský, R., 2019. The on field differentiation of snow avalanche- and debris flow-induced scars in trees as a fundament for improving dendrogeomorphic sampling strategy (case study from the Great Cold Valley in High Tatra Mountains). Cold Reg. Sci. Technol. 158, 1–9. https://doi.org/10.1016/j.coldregions.2018.11.004.
Smith, L., 1973. Indication of snow avalanche periodicity through interpretation of vegetation patterns in the North Cascades. In: Methods of Avalanche Control on Washington Mountain Highways–Third Annual Report. Washington State Highway Commission Department of Highways, Washington, pp. 55–101.
Sorg, A., Bugmann, H., Bollschweiler, M., Stoffel, M., 2010. Debris-flow activity along a torrent in the Swiss Alps: Minimum frequency of events and implications for forest dynamics. Dendrochronologia 28, 215–223. https://doi.org/10.1016/j.dendro.2009.11.002.
Speckman, P.L., Sun, D., 2003. Fully Bayesian spline smoothing and intrinsic autoregressive priors. Biometrika 90, 289–302. https://doi.org/10.1093/biomet/90.2.289.
Stoffel, M., Bollschweiler, M., 2008. Tree-ring analysis in natural hazards research – an overview. Nat. Hazards Earth Syst. Sci. 187–202.
Stoffel, M., Corona, C., 2014. Dendroecological Dating of Geomorphic Disturbance in Trees. Tree-Ring Res. 70, 3–20. https://doi.org/10.3959/1536-1098-70.1.3.
Stoffel, M., Perret, S., 2006. Reconstructing past rockfall activity with tree rings: Some methodological considerations. Dendrochronologia 1–15.
Stoffel, M., Bollschweiler, M., Hassler, G.-R., 2006. Differentiating past events on a cone influenced by debris-flow and snow avalanche activity – a dendrogeomorphological approach. Earth Surf. Process. Landforms 31, 1424–1437. https://doi.org/10.1002/esp.1363.
Stoffel, M., Bollschweiler, M., Butler, D.R., Luckman, B.H., 2010. Tree Rings and Natural Hazards: A State-Of-The-Art. Springer.
Stoffel, M., Corona, C., Guillet, S., Trappmann, D., 2016a. Räumlich-zeitliche Rekonstruktion der Lawinenaktivität am Standort Oberwald, Obergoms, Kanton Wallis, Schweiz. Technischer Bericht 1, vol. 37. Labor für Dendrogeomorphologie, University of Bern, Bern, Switzerland.
Stoffel, M., Corona, C., Trappmann, D., Guillet, S., 2016b. Räumlich-zeitliche Rekonstruktion der Lawinenaktivität im Goms Münster-Geschinen, Kanton Wallis, Schweiz. Technischer Bericht, vol. 2. Labor für Dendrogeomorphologie, University of Bern, Bern, Switzerland, 35.
Szymczak, S., Bollschweiler, M., Stoffel, M., Dikau, R., 2010. Debris-flow activity and snow avalanches in a steep watershed of the Valais Alps (Switzerland): Dendrogeomorphic event reconstruction and identification of triggers. Geomorphology 116, 107–114. https://doi.org/10.1016/j.geomorph.2009.10.012.
Tanner, M.A., 1992. Tools for Statistical Inference: Observed Data and Data Augmentation Methods. Springer-Verlag.
Tichavský, R., Šilhán, K., Stoffel, M., 2017. Age-dependent sensitivity of trees disturbed by debris flows – Implications for dendrogeomorphic reconstructions. Quat. Geochronol. 42, 63–75. https://doi.org/10.1016/j.quageo.2017.09.002.
Todea, C., Pop, O.T., Germain, D., 2020. Snow–avalanche history reconstructed with tree rings in Parâng Mountains (Southern Carpathians, Romania). Rev. Geomorfol. 22, 73–85. https://doi.org/10.21094/rg.2020.099.
Torrenté, A., 1888. Les forêts et les avalanches de la vallée de Conches en Valais. Jahrb. Schweiz. Alpenclub 336–338.
Trappmann, D., Stoffel, M., 2013. Counting scars on tree stems to assess rockfall hazards: A low effort approach, but how reliable? Geomorphology 180–181, 180–186. https://doi.org/10.1016/j.geomorph.2012.10.009.

Trappmann, D., Corona, C., Stoffel, M., 2013. Rolling stones and tree rings: A state of research on dendrogeomorphic reconstructions of rockfall. Prog. Phys. Geogr. 37, 701–716. https://doi.org/10.1177/0309133313506451.

Tumajer, J., Treml, V., 2015. Reconstruction ability of dendrochronology in dating avalanche events in the Giant Mountains, Czech Republic. Dendrochronologia 34, 1–9. https://doi.org/10.1016/j.dendro.2015.02.002.

Van der Burght, L., Stoffel, M., Bigler, C., 2012. Analysis and modelling of tree succession on a recent rockslide deposit. Plant Ecol. 213, 35–46. https://doi.org/10.1007/s11258-011-0004-2.

Voiculescu, M., Onaca, A., 2013. Snow avalanche assessment in the Sinaia ski area (Bucegi Mountains, Southern Carpathians) using the dendrogeomorphology method: Snow avalanche assessment in the Sinaia ski area. Area 45, 109–122. https://doi.org/10.1111/area.12003.

Voiculescu, M., Onaca, A., 2014. Spatio-temporal reconstruction of snow avalanche activity using dendrogeomorphological approach in Bucegi Mountains Romanian Carpathians. Cold Reg. Sci. Technol. 104– 105, 63–75. https://doi.org/10.1016/j.coldregions.2014.04.005.

Voiculescu, M., Onaca, A., Chiroiu, P., 2016. Dendrogeomorphic reconstruction of past snow avalanche events in Bâlea glacial valley–Făgăraş massif (Southern Carpathians), Romanian Carpathians. Quat. Int. 415, 286–302. https://doi.org/10.1016/j.quaint.2015.11.115.

Wahba, G., 1978. Improper Priors, Spline Smoothing and the Problem of Guarding Against Model Errors in Regression. J. R. Stat. Soc. Ser. B Methodol. 40, 364–372. https://doi.org/10.1111/j.2517-6161.1978.tb01050.x.

Wikle, C.K., 2003. Spatio-temporal models in climatology. In: Encyclopedia of Life Support Systems (EOLSS), Developed under the Auspices of the UNESCO. Eolss Publishers, Oxford, UK.

Wikle, C.K., Berliner, L.M., Cressie, N., 1998. Hierarchical Bayesian space-time models. Environ. Ecol. Stat. 5, 117–154. https://doi.org/10.1023/A:1009662704779.

Zgheib, T., Giacona, F., Granet-Abisset, A.-M., Morin, S., Eckert, N., 2020. One and a half century of avalanche risk to settlements in the upper Maurienne valley inferred from land cover and socio-environmental changes. Global Environ. Change 65, 102149. https://doi.org/10.1016/j.gloenvcha.2020.102149.

Zgheib, T., Giacona, F., Morin, S., Granet-Abisset, A.M., Favier, P., Eckert, N., 2022b. Diachronic quantitative snow avalanche risk assessment as a function of forest cover changes. J. Glaciol. 1–19. https://doi.org/10.1017/jog.2022.103 (in press).

Zielonka, A., Wrońska-Wałach, D., 2019. Can we distinguish meteorological conditions associated with rockfall activity using dendrochronological analysis? - An example from the Tatra Mountains (Southern Poland). Sci. Total Environ. 662, 422–433. https://doi.org/10.1016/j.scitotenv.2019.01.243.